Bull. Spec. Astrophys. Obs. 1994, **38**, 58-102.
520.272.2:520.88

RATAN-600 RADIO TELESCOPE IN THE "ZENITH" MODE

YU.N.PARIJSKIJ, O.V.VERKHODANOV, G.A.PINCHUCK,
A.T.BAJKOVA, A.YA.GOL'NEV, N.A.ESEPKINA,
YU.K.ZVEREV, E.K.MAJOROVA, M.G.MINGALIEV,
L.V.OPEIKINA, A.A.STOTSKIJ, A.V.TEMIROVA,
P.A.FRIDMAN
Special Astrophysical Observatory of the Russian AS,
Nizhnij Arkhyz 357147, Russia

ABSTRACT. *A detailed description of the mode "Zenith" or t near-zenith synthesis mode of operation of the RATAN-600 radi telescope is presented. In this mode the radio telescope operated with the ring aperture. The ideology, construction features, and electrodynamic characteristics of this mode a discussed. Fundamental astrophysical problems and methods their solution are considered. Adjustment observations, mappi of the radio galaxy Cignus-A, and two-dimensional sky surv at a declination of 47° are described. Basic results of the observations are given. Performance of the RATAN-600 for years in the "Zenith" mode is summarized. Future possibiliti of performance in this mode are considered. These are: tracki objects with a moving observation cabin, performance of t RATAN- 600 as an antenna array, "3-dimensional" radi astronomy, and "patrol" observations.*

INTRODUCTION

The primary goal of the variable profile antenna (VPA) radio telescope was to get at least a one-dimensional resolution and large collecting areas (Khaikin & Kaidanovskij, 1959).

Elimination of purely mechanical restrictions in an ordinary radio telescope of 150-200 m in diameter enabled the discussion of systems with a one-dimensional resolution of about 1″ and collecting area of more than 10^6 m^2 (Khaikin et al., 1967). However, it became clear at the end of the 50s that the problem of two-dimensional imaging can be solved with VPA antennae too (Parijskij, 1961).

Several variants of radio imaging were proposed in the RATAN-600 project (Parijskij & Shivris, 1972): "consecutive" azimuth synthesis, circumpolar synthesis, and "parallel" near zenith synthesis. The most universal one is the azimuth synthesis for in this case the larger part of the sky visible with the telescope can be synthesized (see Minchenko, 1977; 1978; 1979 for the first observations and algorithm). One can observe the least sky region in the circumpolar synthesis mode but with the maximum integration time. The azimuth synthesis with the flat reflector is apparently necessary for the mapping of objects with considerable negative declinations, i.e. Galaxy centre and lower than that (Minchenko, 1986; Gelfreikh and Opeikina, 1992).

However, both the best resolution and largest collecting area are achieved in the near-zenith synthesis with the use of the entire antenna ring aperture. When observing objects using the consecutive synthesis of their Fourier images, by filling the UV-plane, as a result of observations at different azimuths, the radio telescope aperture is used less effectively than for parallel synthesis observations in the near-zenith direction (Parijskij and Shivris, 1972; Parijskij, 1986). So the region shown in Fig. 1a is synthesized with four independent sectors, while a circle with the radius D/λ on the UV-plane is synthesized in parallel synthesis (Fig. 1b).

A special observation cabin is used in this mode of operation at the RATAN-600. This observation cabin is a combination of a conic and parabolic mirrors (Figs. 2,3), and is of type VI (six). A shift of the cabin in the horizontal plane and a change of the main ring reflector shape (by radial displacement of elements limited to ±0.5 m) permits us within certain limits to vary the observational direction.

Since the observation cabin was put into operation autocollimation adjustment has been made by Dibizhev et al. (1986), the radio sources 3C84 and Cygnus-A have been

synthesized, and a two-dimensional survey has been carried out (Mingaliev et al. 1991). Performance features of the radio telescope in the "Zenith" mode will b described below. Some observational results will be given and the problems of th radio telescope operation in this mode will be considered.

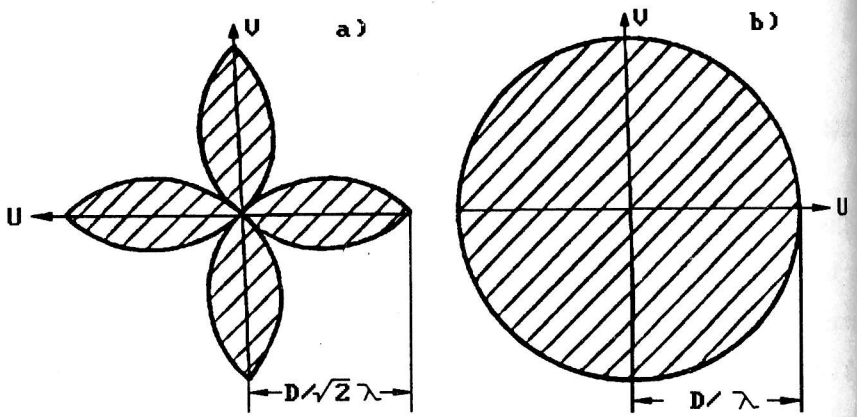

Fig.1. **a)** *Filling of the UV-plane in the consecutive synthesis imaging with the 4 sectors.* **b)** *Concurrent near-zenith synthesis.*

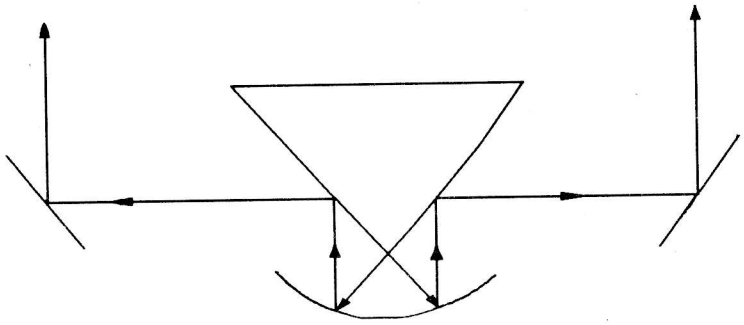

Fig.2. *The path of rays in the three-mirror system (a conic and two parabolic mirrors).*

IDEOLOGY AND CONSTRUCTIONAL FEATURES OF THE OBSERVATION CABIN NO.VI

Superposition of electric fields reflected by the surface elements occurs in th focus of any radio telescope. The basic information is in pairs of the products o E_i and E_j fields since the square magnitudes are registered. Therefore it is easy t show that the square filter of the ring aperture has a non-zero sensitivity every where in a circle of radius D/λ, where D is the diameter of the RATAN-600. The sensi tivity of the UV-plane was calculated in a manner of "island diagram" described i the paper of Parijskij (1969). The Muller matrix and the filter form have been explo red in the paper by Kuznetsova (1973). A strict analytical expression for the spatia frequency response function of the RATAN-600 in Zenith, taking into account the limi ted radiometer band, is shown both below and in Fridman (1985).

If we consider small ring widths the field diagram in the scalar approximation i automatically specified because the Fourier transformation from $\delta(r-a)$ is propor tional to $J_0(\theta)$.

But, difficulties arise in the vector consideration. As was detected by Sobolev and theoretically explained by Kuznetsova and Soboleva (1964), a large part of th energy disappears when illuminating the ring aperture by vertical or horizontal po

larization. Parijskij (1969) proposed to overcome these difficulties using a three-mirror system, where the first mirror was a typical paraboloid and the other two reflectors in combination gave a transformation with a unit matrix of the flat wave vector field in the paraboloid aperture. This case is shown in Fig. 3 (for more details see the paper by Esepkina and Parijskij (1972)). Here we note that the vector field of the primary horn in the spherical wave in geometrical optics approximation is transferred without distortions to the main reflector aperture. The polarization structure of the field will have a different character at different azimuths in the cylindrical wave in the experimental investigation of the main mirror illumination.

Besides, the absence of illumination symmetry in the E and H planes will show up in the autocollimation manner of field distribution in aperture measurement. In conclusion, reflectors which are completely symmetrical in the E and H planes do not give cross-polarization on the parabolic mirror (Esepkina et al., 1973), and hence the primary feed field will not be changed in the RATAN-600 aperture.

Thus, for the zenith mode we have chosen an observation cabin, which is a combination of a conic and a parabolic reflectors (Fig. 2). The size of the observation cabin is specified in Esepkina and Parijskij (1972):

1) The length of the cone generant must be equal to the height of a reflecting element h;

2) The cone height = $h \cdot \cos 45^\circ$;

3) The cone base = $2h \cdot \cos 45^\circ$;

4) The diameter of the paraboloid of rotation is $d_0 = 2h \cdot \cos 45^\circ$.

Mechanical properties of the type VI observation cabin (movement in the antenna field) are similar to those of other observation cabins (Amstislavskij et al., 1972).

The possibility of tracing an object is realized in the design of this cabin. In this case the carriage of the cabin moves along the arc rails incorporated in the structure of the cabin. The integration time in the tracing mode is a little less than a minute (this mode is considered in more detail below).

ELECTRIC AND DYNAMIC CHARACTERISTICS OF A VPA IN THE ZENITH MODE

The minimum elevation for possible parallel synthesis with the total circle is defined from the following expression:

$$\cos \theta_{0_{min}} = \sqrt{\frac{2C}{R+C} + \left(\frac{C}{R+C}\right)^2}, \qquad (1)$$

where R is the radius of the VPA, $C = \Delta R_{max}$ is a maximum possible radial shift of elements equal in our case to $3 \cdot 10^{-3} R$. That is why

$\theta_{0_{min}} = 85^\circ 30'$.

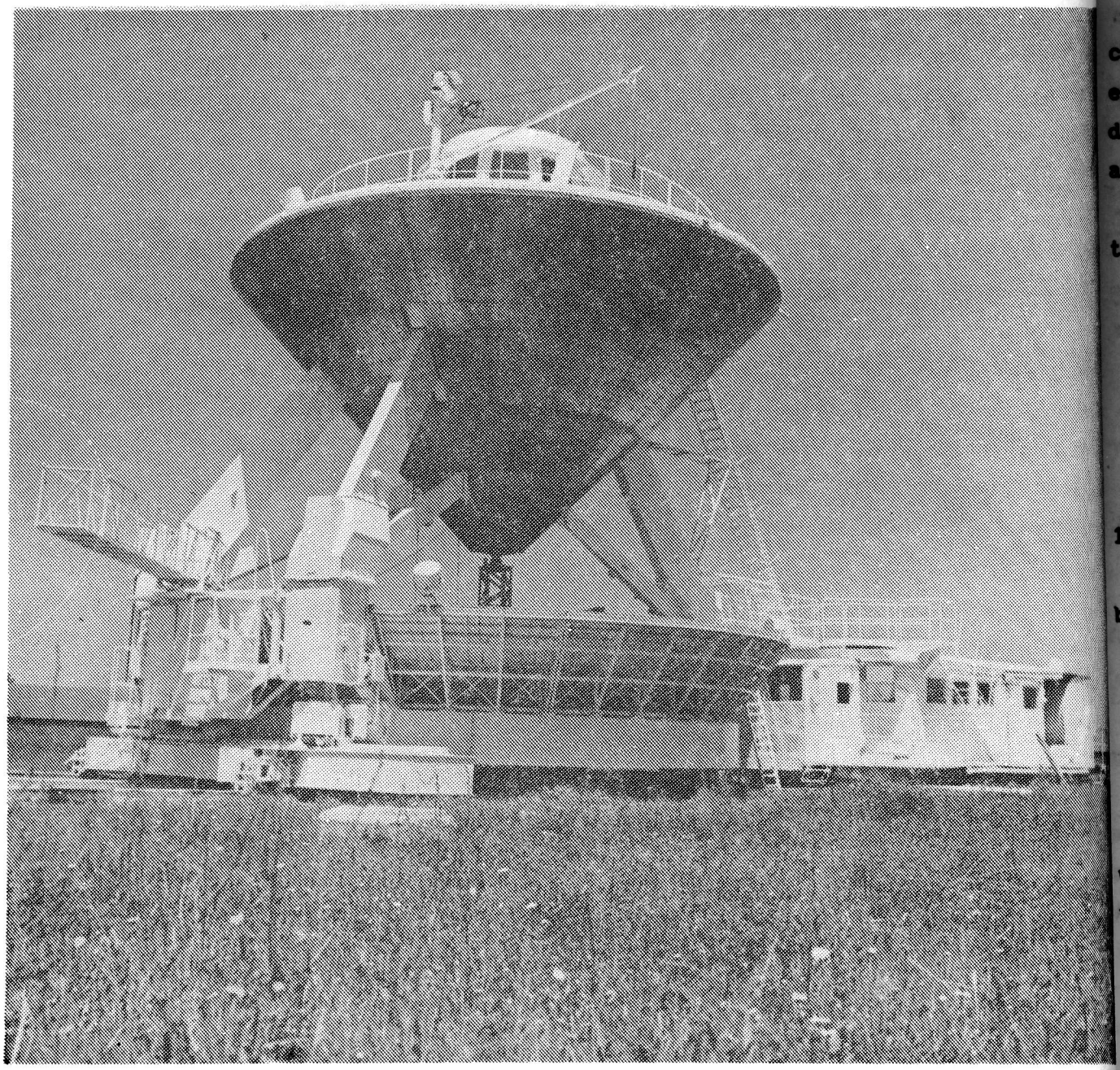

Fig.3. *The observation cabin of type VI.*

Thus, when all the reflecting elements of the RATAN-600 are illuminated, it is capable of receiving radio signals from a strip limited by an angle of ±4.5 degrees in elevation. In this case the width of the power beam pattern (BP) at the level 0.5 is specified by the diameter of the total ring aperture (D = 576 m). It will be equal to $\cong 0.726\ \lambda/D$ if we consider the antenna as an infinitely thin ring (Fridman, 1985). The beam pattern in this approximation has circular symmetry. The dependence on the radial coordinate is given by the following formula:

$$A(\theta) = J_0^2 \left(\frac{\pi D}{\lambda} \theta \right). \qquad (2$$

Thus, $\theta_{0.5}$ = 21″ at the length λ = 8.0 cm.

The limited ring width, non-zero receiver bandwidth, and finite height of the secondary mirror should be considered in the VPA BP calculation in a tough case. The effect caused by the limited size of the secondary mirror can be ignored because the diameter of the field of view defined by this effect at our wavelength (8 cm) is approximately equal to 180 beams (Fridman, 1985).

The beam pattern, with allowance for the limited ring width, can be computed by the following formula:

$$A(\theta) = \frac{1}{(1-\varepsilon^2)^2}\left[\frac{2J_1(u)}{u} - \varepsilon^2\frac{2J_1(\varepsilon u)}{\varepsilon u}\right], \qquad (3)$$

where $\varepsilon = \frac{D-h}{D+h} = 0.9823$, $h = \cos H \cos\varphi$, H is the height of the elements (7.4 or 11.4 m), $\varphi \cong 45^\circ$, and $u = \pi D\theta/\lambda$.

In the case of non-zero receiver bandwidth the BP must be integrated with the bandwidth:

$$A_{\Delta f}(\theta) = \frac{1}{\Delta f}\int_{f_0-\frac{\Delta f}{2}}^{f_0+\frac{\Delta f}{2}} A(u/c)K(f)df, \qquad (4)$$

where $K(f)$ is the amplitude frequency characteristic of the receiver, c, the light velocity, f_0, the central frequency of the receiver.

Fig. 4a shows the beam patterns of the ring with a limited bandwidth. In Fig. 4b (curves 2, 3) are displayed the spectra $\tilde{A}(u)$ for 5% and 10% bandwidths.

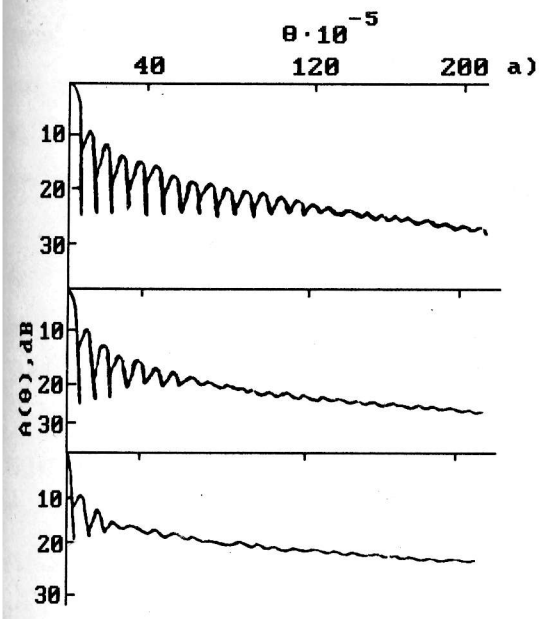

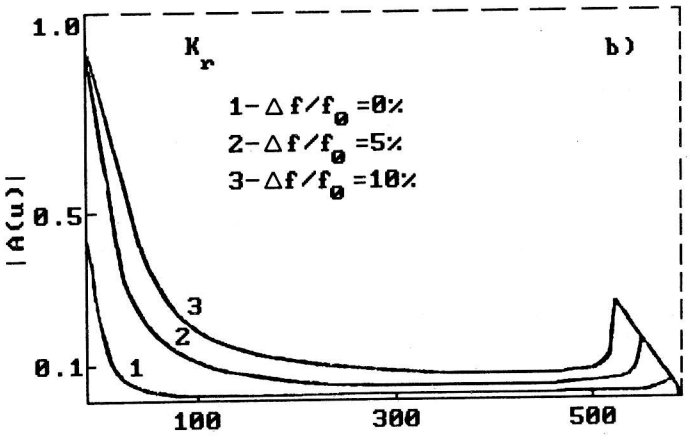

Fig.4. a) *The beam patterns in the circular aperture operation mode with the account of the finite bandwidth* Δf.
b) *The* $\tilde{A}(u)$ *spectra for different bandwidths.*

As shown by Fridman (1985) the limited bandwidth and limited ring aperture widt "wash off" beam pattern lobes and raise the level of spatial harmonics in the middl of the spectrum ($h < u < D-u$), the influence of the band being stronger. One has t allow for this when computing the optimum criterion $K_{opt}(u)$ in the data processing.

The "washing off" of the BP side lobe structure can be avoided if the wide ban input of the radiometer at the output of ultra-high frequency (UHF) amplifier is di vided by the N channels with the band $\Delta\nu < H/R$. Each narrow channel will create H $J_0(ax)$ of different scales. With the further data processing these partial beam can be reduced to one scale and summarized. In this case the function $J_0(ax)$ will b confined only by the BP of the element λ/H.

CALCULATED PARAMETERS OF THE RATAN-600 IN THE ZENITH MODE

Calculation of the parameters (noise temperature T_n and effective area of the ra dio telescope S_e) for Zenith operation of the RATAN-600 is described in the paper o Majorova and Stotskij (1986) for the wavelengths from 2 to 21 cm.

The diameter of the ring aperture is 576 m. With the element as high as 7.4 m th width of the aperture was 5.23 m and the geometrical area was 9464 m^2. When th height of the element was increased to 11.4 m (in 1992) the ring aperture width an area became 8 m and 15000 m^2, respectively. Table 1 shows the results of computin T_n, S_e, and values $G=S_e/T_n$ characterizing the efficiency of the radio telescope, a is the height of the element.

It is interesting to estimate how efficient are the enlargement of the element from 7.4 to 11.4 m and the use of radiometers with a low-level intrinsic noise (20 K) (Berlin et al., 1982). The ratios of the values of $G(a_0, T_r)$ calculated fo different combinations of a_0 and T_r are given in Table 2.

Table 1.

λ	a_0	a_e	T_r	T_a	T_n		S_e	G	
					T_r =20K	T_r =100K		T_r =20K	T_r =100K
cm	m	m	K	K	K	K	m^2	m^2/K	
21	7.4	2.0	135	142	162	242	3330	21	14
	11.1	4.0	99	112	132	212	6659	50	32
8	7.4	3.7	52	68	88	168	6218	71	37
	11.1	5.2	19	37	57	137	8705	152	64
4	7.4	4.0	17	35	55	135	6572	119	49
	11.1	4.5	4	23	43	123	7395	172	60
2	7.4	4.1	6	25	45	125	6485	144	52
	11.1	4.1	1	20	40	120	6485	162	54

Thus, one can see that both the enlargement of the elements and the reduction

radiometer noise improves the efficiency of the radio telescope. The first greatly improves the efficiency at long wave observations, and the second at short wave observations. This fact was confirmed by the measurements made in 1992 (Majorova et al., 1993).

Table 2.

λ, cm	$\frac{G(11.1\ m;\ T_r)}{G(7.4\ m;\ T_r)}$		$\frac{G(a_0;\ 20K)}{G(a_0;\ 100K)}$		$\frac{G(11.1m;\ 20K)}{G(7.4m;\ 100K)}$
	T_r =20K	T_r =100K	a_0=7.4m	a_0=11.1m	
21	2.4	2.3	1.5	1.6	3.6
8	2.1	1.7	1.9	2.4	4.1
4	1.1	1.2	2.4	2.9	3.5
2	1.1	1.0	2.8	3.0	3.1

GEODESIC ADJUSTMENT OF THE TYPE VI OBSERVATION CABIN

The geodesic manner of adjustment was used to form the reflecting surface of the parabolic and conic mirrors.

The surface of the parabolic reflector was formed in the standard wide-spread manner with the help of the flag-templet (Fig.5a). In this case the vertical rotation axis of the templet was matched with the centre of the parabolic mirror and with a point at the top of the conic one. The working edge of the templet was adjusted after its installation in the bowl of the mirror using special marks. These marks were set along one of the cross-sections strictly by parabola with high precision leveling and linear measuring. The mirror was horizontalled by the level which was set on the templet. The surface was formed by setting a selected gap between the working edge and the adjusted cross-section of the surface. The surface elements were displaced with screws fixed simultaneously. The check was made by the prober allowing to fix deviations from the project gap with an accuracy of 0.02 mm.

After the adjustment was finished the checking measurements of the adjusted surface were made with the high precision levelling. According to the results of these measurements the accuracy of the surface is characterized by the root-mean-square (rms) error of about 0.2 mm.

The conic reflector surface was formed in the manner worked out specifically for this case. Its essense is that a standard conic surface is formed by rotation around the cone axis of a string stretched at a 45° angle to it (Fig. 5b). One end of the string is fixed to a point on the cone axis at the top of the standard cone, the other end is fixed to a point on the rotated boom. The vertical axis of this boom coincides with both cone and observation cabin axes. Essential angle of the string

incline to the cone axis is given by the displacement into different directions o point of the string fastening to the rotated boom. In this case the surface formed by setting the selected gap between the string and the adjusted cross-sect of the surface. The gap is checked by the optics-mechanical micrometer graduated 0.01 mm. After the adjustment was finished the checking measurements were again m in the same manner. According to the results of these measurements the surface error is less than 0.3 mm.

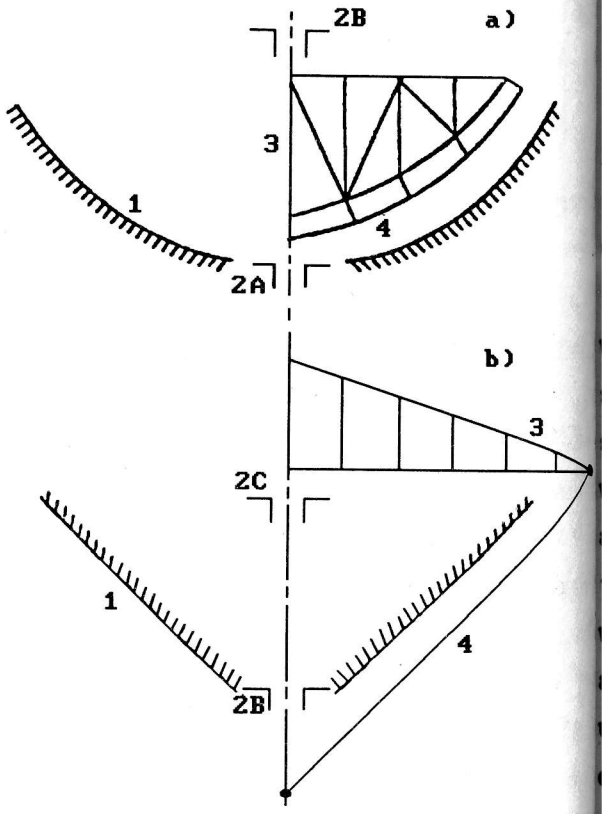

Fig.5. *A schematic of geodesic adjustment of observation cabin VI.*
a) *1 - the parabolic mirror surface, 2A and 2B - the sleeves presetting the parabolic axis, 3 - a flag-templet, the working frame of the templet;*
b) *1 - the conic mirror surface, 2B and 2C - the sleeves presetting the cone axis coincident with the paraboloid axis, 3 - the rotating bar, 4 - the string.*

AUTOCOLLIMATION ADJUSTMENT OF THE RATAN-600 IN THE "ZENITH" MODE

The adjustment of the elements consisted in defining the positions at which t form a sector of a circular cylinder. The obtained initial positions of the eleme are further used in the antenna setting calculation for radio astronomical obse ations (Dibizhev et al., 1986).

A horn of a very high frequency (VHF) apparatus for special adjustment is inst led in the focus of the system for autocollimation (AC) adjustment. This horn e short impulses in the direction of the main reflector elements (Stotskij et a 1987). The emitted energy is gathered by this horn again after it has been refle from the panels. In the angular coordinates the elements are adjusted the maximum of the reflected signal and in the radial coordinates by phase compa ting with a reference panel. Reference elements can be preliminarily set in a ge

sic way.

The main reflector adjustment for observations was executed in two stages.

At the beginning all 4 sectors were adjusted by the usual AC method, using the observation cabin intended for observations with one sector (observation cabin No. 2). The adjustment was performed at a wavelength of 3 cm with the standard adjustment apparatus. Twelve panels set earlier in a geodesic manner in a circle with a radius of 288000.0 mm were used as reference ones. AC focal spots at the waves 3 cm and 8 mm and AC efficiency, which characterizes the ratio of power reflected in the AC mode to the total emitted power, showed satisfactory quality of adjustments.

Radio holography measurements of element positions (Pinchuk and Stotskij, 1982) permitted evaluation of the quality of "junctions" of sectors. They gave satisfactory results from radio holography data. The rms error for the alignment of elements was 0.3 mm.

At the second stage the panel positions were accurately defined by the AC method with the use of the type VI observation cabin. The adjustment apparatus used at this stage was designed on the basis of the cabin radiometer (wavelength 8.0 cm). The standard generator G4-81 was used. A special impulse device with improved parameters was also created because the difference between emitted and received signals for adjustment of the entire ring must be at least 16 times better in comparison with that of one sector. Adjustment carried out with the type VI observation cabin at the wavelength coincident with the wave of observations allowed us to bring the adjustment conditions much closer to those of observations. In particular, it allowed us to take into account the phase delays in the two-mirror system of the observation cabin and the effect of pylons supporting the conic mirror.

A comparison of the results of adjustments carried out with different cabins showed that the initial set of elements changed appreciably after the transition from observation cabin II to VI (Fig.6). The biggest radial shifts were observed in the regions obscured by the pylons. In this case the displacement of the elements reached 10-15 mm. It was caused by diffraction of electromagnetic waves on the pylons. The shifts were smaller in the remaining part of the ring mirror. Their rms value (without taking into account large-scale components) was 0.7 mm. These shifts are likely to be frequency-dependent and partially associated with the difference in geometry of the cabin mirrors. They are also due to the limited accuracy of adjustments. Usually the difference in positions of radial panels after two AC adjustments was about 0.3 mm (Stotskij et al., 1987). It could be a little larger for these measurements because the accuracy of adjustment with the type VI cabin was weaker due to the longer wavelength and longer adjusting time.

AC focal spots measured at the wavelength 8 cm with a displacement of the observation cabin in the directions North-South and East-West are shown in Fig. 7. The level of sidelobes and the width of the main lobe correspond to the calculations if one accounts for the field distribution along the main reflector.

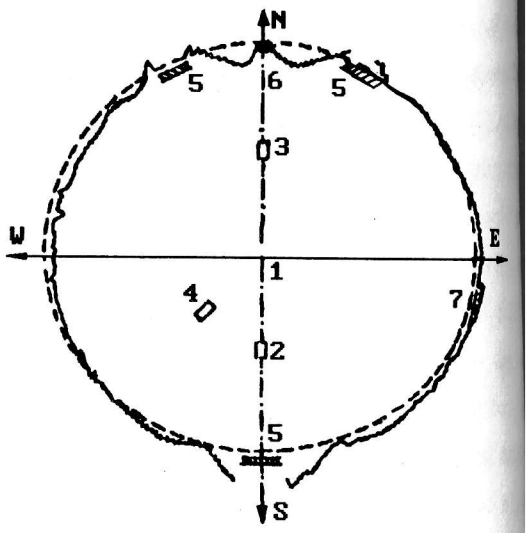

Fig.6. *Comparison of the results of the adjustment executed with observation cabin III and IV. 1 - the focus position of observation cabin VI; 2, 3 and 4 - the locations of observing cabins I,II and III; 5 - the regions of the geometrical "shadow" of the pylons; 6 - the "shadow"of observation cabin II; 7 - the group of unused panels.*

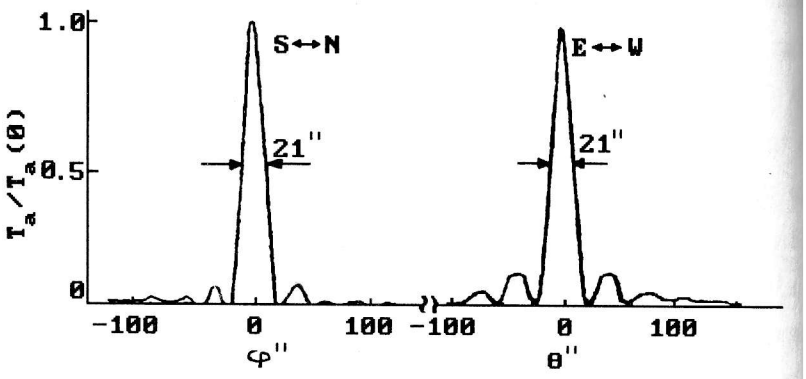

Fig.7. *The longitudinal and transversal AC focal spots.*

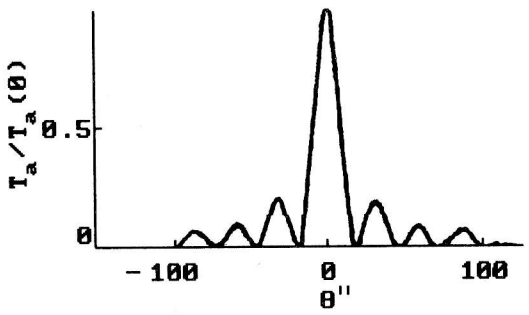

Fig.8. *The curve of transit of the radio source 3C84 on January 29 1986.*

Finally the quality of adjustment and radio telescope parameters when working wi the entire ring aperture were checked in the radio astronomical observations of t source 3C84. A transit curve across the BP (cross-section East-West) is shown in Fi 8. The effective collecting area of the radio telescope defined from these obser ations is 3000 m^2. This value is close to the one computed by Majorova and Stotsk (1986) under the following conditions: the effect of the Earth is taken in account, the main mirror panels obscured by the pylons and observation cabins II a III, and 50 panels unused for technical reasons, are excluded (Fig. 6). The angul resolution of the radio telescope with the use of the entire ring aperture w 21"x21".

Regular radio astronomical observations in the Zenith mode were started aft these adjustments.

INVESTIGATION OF THE FIELD DISTRIBUTION OVER THE MAIN MIRROR FOR THE NEAR-ZENITH MODE OF ANTENNA OPERATION

A conic cabin was mounted in the centre of the antenna at the distance R=288 m for measurement of the vertical field distribution near the main mirror. Over the entire ring measurements were made for each 30° in azimuth. The panels were set vertically in this case. A semiconductor modulated noise generator with an amplifier was used as a measuring generator. It was elevated from 0 m to 9 m with a crane (located near to the elements). The zero height mark was made coincident with the lower edge of a panel in each measurement of a new azimuth. A signal was received using a standard radiometer at the wavelength 8.0 cm with a VHF amplification of 60-65 dB and a detector bandwidth Δf = 450 MHz (see below). A quasi-scalar primary feed having a sufficiently symmetrical BP in the E and H planes and a low level of the lateral radiation (Fig. 9) was used as a primary feed.

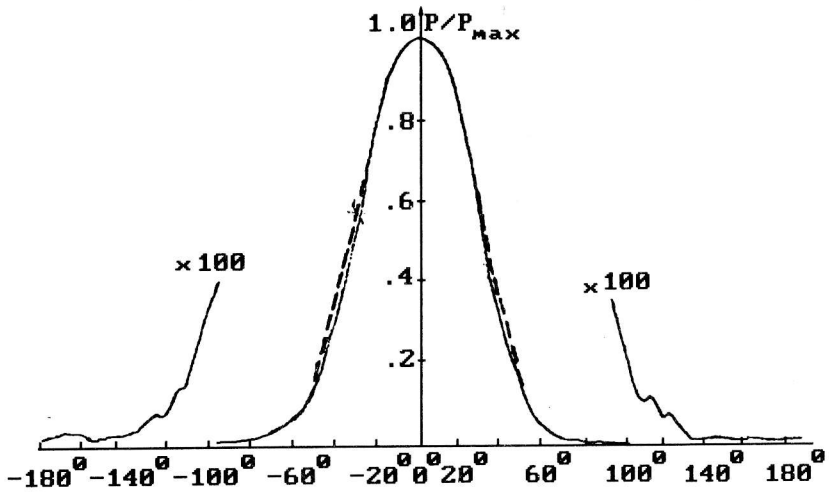

Fig.9. *The beam pattern of the primary feed. The solid line being for the H-plane, the dashed line for the E-plane.*

The field and power distributions over the element are shown in Fig. 10. The panels of 2 m x 7.4 m were set at an angle of 45° in the observations in Zenith. Real illumination borders are shown by the dot/dash line in Fig. 10.

It is obvious from the picture that overillumination is from the vertical and the use of additional screens (i.e. 1 m panels lengthening both sides) will essentially decrease this effect and increase antenna effective area. The power distribution over the element at various shifts of the primary feed along the focal axis of paraboloid of rotation is shown in Fig. 11.

Besides, the field distribution in the cylindrical front along the conic reflector was measured (Fig. 12). In this case a standard noise generator was lifted vertically with a standard crane installed on the upper plane of the cone. The five-metre mark coincides with the base of the conic reflector of 4.8 m in height.

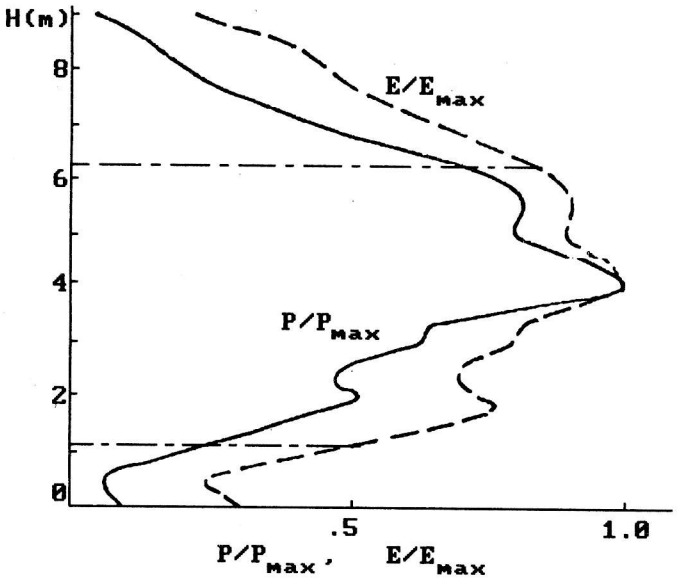

Fig.10. *The field and power distribution in height. The dash-and-dot line shows the limits of illumination of a panel.*

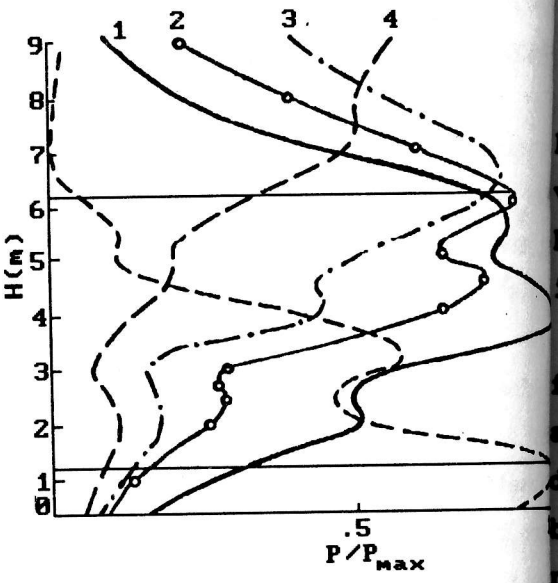

Fig.11. *The field distribution in height near the main mirror at different shifts Δ of the primary feed along the focal axis of the paraboloid. Curve 1 refers to the shift Δ=0, curve 2 Δ ≅ -λ/4, curve 3 Δ ≅ λ/2, curve 4 Δ ≅ -λ, curve 5 Δ ≅ +λ. The limits of the panel projection (from 1.1 m to 6.3 m) are also shown.*

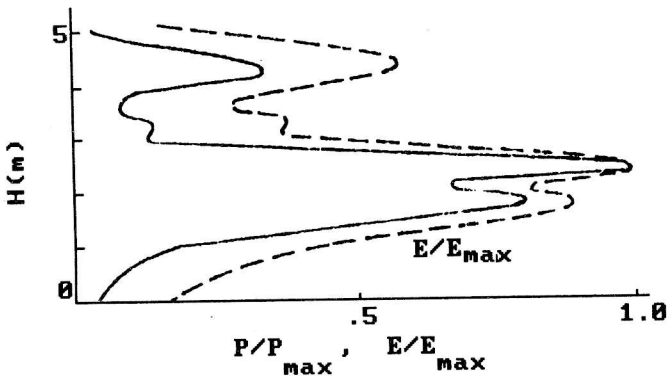

Fig.12. *The field distribution in the cylindrical wave near the conic reflector. The 5 m mark corresponds to the cone bas*

ASTROPHYSICAL TASKS FOR THE OBSERVATION CABIN NO.VI

Astrophysical problems for the "Zenith" mode of operation of the RATAN-600 ha been already discussed by Parijskij (1986). Therefore we will follow the ideology that paper.

Consider consecutively some classical ideas of thought and actual problems of t present time.

a) Synthesis imaging of individual sources

This is a classical problem for radio astronomy. However, taking into account t

great amount of observations carried out with systems of aperture synthesis one has to be careful in selecting objects for investigation.

Apparently, it is necessary, first of all, to explore new objects detected in the RATAN-600 surveys. To save time it is more convenient from the methodical point of view to have wide lists of objects since about 100 objects can be observed per day. However tens of days are needed for each image irrespective of the number of objects in the list.

Here we note that rough estimation of the object structure of model solution type for double structure radio galaxies is possible from the analysis of a single transit across the BP. Let us assume that we observe a double structure radio galaxy at a distance of a few λ/D from the beam axis. Transit of the source across a multilobe beam gives information identical to that obtained with a two-elements Ryle interferometer as a result of the 12h synthesis when tracking an object near the Pole, i.e. we cut out the ring zone from the Fourier image, and simple model schemes are readily analysed (position and amplitude of components, position angle of the major axis etc.). The mean angular size of a source even for faint sources is close to 12″, i.e. it is larger than λ/D for short centimetre waves in the "Zenith" mode, and the largest extragalactic radio sources, as a rule, exceed the RATAN-600 BP λ/D in size. This is just the case needed for such an analogy. This example is shown in Fig. 13.

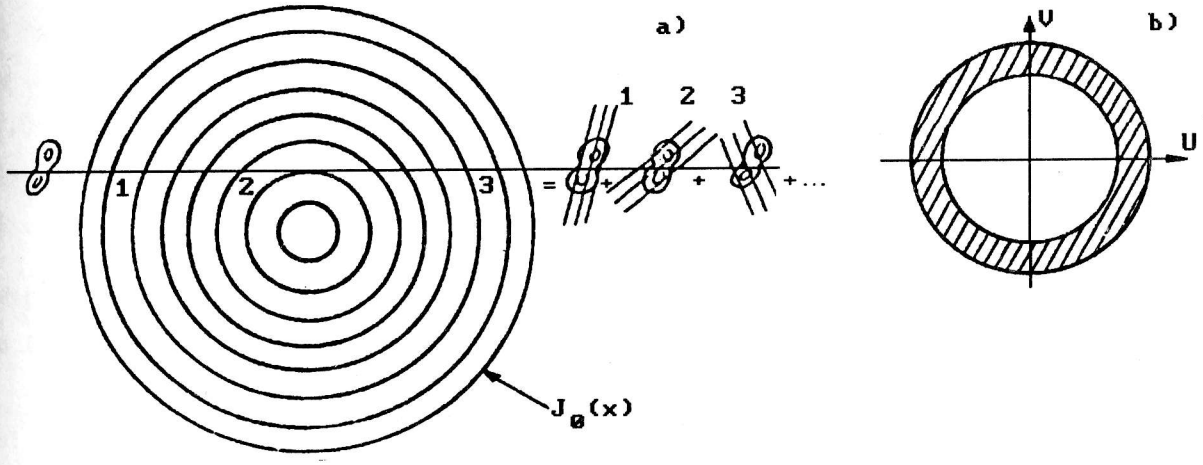

Fig.13. a) *The off-axis transit of a radio source at the Zenith via the function* $J_0^2(x)$ *yields information close to the consecutive synthesis imaging near the Pole with a two-element interferometer. The positions of the sidelobes at points 1,2,3 are shown as an example.*

b) *The UV-plane region registered in a one-time transit of a source.*

The sensitivity of near-zenith synthesis in the "by-list" observational mode depends on the progress of deep radio telescope cooling and the ability to realize a long integration time. It depends also on the efficiency of cleaning the survey of confusion effects (for the efficiency of the "by-list" observation see below).

The work on radio telescope cooling through the shielding of the Earth's radiation

is now in progress (for calculations on the effects see the paper of Korolkov et al. (1978)). It was found that the Earth contribution can be reduced to that of the microwave background. The use of cooled radiometers allows us to count on the creation of detecting and measuring systems with parameters close to ideal, and comparable at the input with both the Earth and sky noise. Let T_{sys}=20K be a limiting estimate of the system temperature at the waves 3-8 cm. The radiometer bandwidth may close to 1 GHz. Both parameters give ΔT_{rms} about 1 mK at τ=1 s. The integration time in the transit mode is about 1 s and about 1 min in the "sliding" mode (Mingaliev et al., 1985).

The total time of visibility of a radio source in the RATAN-600 field of view using the entire ring, is about 1^h. Ways of tracking objects during this time are discussed now.

Probably some equivalent of the classical photoguide will be exploited in the future (Parijskij et al., 1986). A controlled autocollimation spot is proposed to be used as such a guide. About 1% of the total number of elements of the main surface can be used for formation of the spot. The simplest method is the combined manner of transposition and sliding. In this case it is possible to accumulate a signal for 5% of the total time the object stays in the near-zenith zone. The corresponding limiting flux density sensitivity for the 3 modes of the signal accumulation with S_e=30 m^2 will be

"transit" (1 s), $P_{rms} \geqslant 1$ mJy

"sliding" (100 s), $P_{rms} \geqslant 100$ μJy

"tracking"(1 hour), $P_{rms} \geqslant 15$ μJy.

The sensitivity can be trebled using additional screens and increasing the height of the secondary mirror. Further sensitivity improvement can only be attained by averaging over many days of observations.

When mapping a sky region comparable with the BP of a single element, even for wide band observations, a radio telescope, as different from interferometric system, has a finite sensitivity not only within the region of $(\lambda/D)^2$ but in the region of $(\lambda/H)^2$ as well, where H is the element projection onto the aperture. Moreover, since $J_0(x) \to \sin x \sqrt{x}$, the integral of each ring lobe does not depend on the distance from the radio telescope axis until the beam of the element begins to affect. Therefore the correct data reduction of dirty maps must provide an additional gain in sensitivity comparable with $(D/H)^{1/2}$ (see also Fridman, 1985).

b) Two-dimensional sky surveys

1) Extragalactic surveys

cope, i.e. with a sufficient density of objects in the sky, is the most informative. A distinctive feature of the near-zenith survey is the fact that, unlike ordinary sky surveys at the RATAN-600, it is the most sensitive (disregarding the small sky region near the World Pole) and two-dimensional. The last fact gives us confidence in obtaining accurate coordinates for the radio sources. The first experience suggests that one can attain an accuracy comparable with 1 arcsec even for the relatively faint objects. The method of the "immovable focus" (Soboleva et al., 1986) is likely to allow to still further advances. The knowledge of the coordinates and structure of a source will considerably increase the reliability of optical identification of radio sources. An accuracy of 100″ is needed for identification with objects of 21^m of the Palomar Sky Survey, and 3″ for identification of deep snapshots of the 6 m telescope with objects of 25^m. One must be prepared for an accuracy of 0.1″ (i.e. 0.3″ x 0.3″) for the extremely deep images up to 29^m with large space telescopes. Note that a number of such "boxes of errors" on the sky in our strip is greater than that of stars in the Galaxy.

As is shown in the paper of Parijskij and Shivris (1972), full use of the entire ring is possible in a region of zenith distances of $\pm 4.^\circ 5$, i.e. in a strip of 9° in declination or within the solid angle $\Omega = 0.4$ sr for the RATAN-600 latitude or in a region of $\pm 18^\circ$ (Ω=2.7 sr) for narrow band surveys with echelonment. The threshold sensitivity of wide band surveys, at least for "dirty" maps, is close to 1 mJy. Let us note that this level is close to the break of the curve *log N - log S*. This level is the limit for centimetre waves in statistical investigations of the most distant structural objects in the Universe. When passing to microjansky the share of distant objects in the surface density of faint sources will be insignificant, and the sky will be covered with nearby low-luminosity galaxies.

Let us estimate the number of objects observed in the survey mode in a region of 0.76 sr:

optical objects to	21^m	- 10^7
	25^m	- $0.4 \cdot 10^9$
	29^m	- $6 \cdot 10^9$
radio sources (to 1 mJy)		- 10^5
infrared sources		- $2 \cdot 10^4$
X-ray sources		- $2 \cdot 10^4$
gamma sources		- 10^2.

Thus in the RATAN-600 field of view there are quite enough objects for various statistical explorations. One survey has already been carried out at the RATAN-600 in the "Zenith" mode.

2) Galaxy

The Milky Way, containing objects of especial interest, crosses the "Zenith" region of the RATAN-600. First of all we see the Galaxy along spiral arms, where the known complexes of star formation, supernova remnants, sources of mazer radiation in

OH and H_2O, planetary nebulae, and one of the brightest and nearest stars, etc. situated.

It is also easy to explore the poorly investigated Galaxy structure at the galactic latitudes, and as a part of it the "ripple" of background radiation dete in the "Cold" experiment (Parijskij and Korolkov, 1986).

Note that the RATAN-600 is unrivalled in sensitivity to background ra tions. Here the RATAN-600 in many respects is close to a combination of parabol and aperture synthesis system. Such a combination, as known, permits the separa of the background radiation from interfering discrete sources. One of the new p lems with the background radiation is the search for one-dimensional formations those recently detected near the Galaxy nucleus. The absence of specific polariza instrumental effects (Parijskij and Shivris, 1972) in the near-zenith synthesis permits us also to work on the problem of polarization exploration of the gala background with a sensitivity unobtainable by other means. This direction is clos related to the problem of the acceleration and diffusion of cosmic rays and to problem of magnetic field origin in the Galaxy. A brightness sensitivity higher t 1 mK with the resolution from 1° to a few arcminutes and higher is needed.

c) Radio spectroscopy

New possibilities for interstellar medium radio spectroscopy arise. Mapping in nes of the Milky Way regions, even moderate in the size, with a resolution of 1′ not been made yet and it may give a surprise. Observations with a resolution of 1′ CO 2.6 mm line may be entirely unpredictable. However, prior to a discussion of short-wave observations we will recall their technical problems.

d) Zenith and mm range

The first and compulsory stage is successfully mastered: the "conveyer" for impr ving the quality of separate main surface elements is already operative. By the b ginning of 1986 about 140 elements had a surface accuracy of 0.082 mm in the centr part of size 5.5 x 2 m. After recalculation to the aperture when observing at the z nith it gives an accuracy of 0.060 mm.

The methods of mutual alignment of elements have also been successfully develope An accuracy of about 0.1-0.07 mm seems real even with the existence of thermal defo mations of the main surface, whose adjustability and controllability allow us to u methods of active optics. Apparently it is sufficient to create a specialized seco dary mirror possibly of smaller sizes than type *VI* and one may expect success. No that the "diagonal errors" in this near zenith mode are equal to 0 and the radii curvature of all the panels are equal. In 1985 a decision was made to make all n elements with an optimum radius of curvature for the near-zenith synthesis. Then t

resolution at the wavelength 2.6 mm would be 0.55″ x 0.55″, and the geometrical area about 5000 m^2. Besides spectral observations, stellar astronomy problems can be posed.

e) Solar radio astronomy

The possibilities of solar observations in the Zenith synthesis mode with the unclosed ring are discussed by Gelfreikh and Opeikina (1992), (see also below about the solar heliograph). Various variants of incomplete use of the ring for strong objects like the Sun have long been proposed by Kajdanovskij (1982).

ZENITH OBSERVATION CABIN RECEIVER

A 3.75 GHz radiometer created by Gol'nev (Gol'nev et al., 1989) is in the focus of the Zenith cabin (Fig.3, Fig.14).

This radiometer is a direct amplification circuit. An uncooled magnetic memory commutator with a loss less than 0.1 dB (Afanasjev and Berlin, 1985) is used as the input "antenna-equivalent" switch.

The first two amplification stages are parametric amplifiers cooled down to 15 K with a microcryogenic system (MCS). The third stage is an amplifier placed in the same cryostat of the MCS with cooling down to 60-70 K (Lebed' and Yaryomenko, 1985, Berlin et al, 1989). The next stage incorporates uncooled amplifiers.

Radiometer balancing before observations and current calibration are made using the semiconductor noise generators. A noise signal is injected to the input waveguide through the directional couplings.

A specially worked out adjustment complex is incorporated in the device. Adjustment of the system "primary feed - secondary mirrors (parabolic and conic)" is peformed with this adjustment apparatus.

The following parameters have been realized in observations:

central frequency f_0=3.75 GHz,
bandwidth Δf=450 MHz,
sensitivity ΔT_{calc}=6.5 mK, ΔT_{fact}=7.0 mK,
system noise temperature $T_{n.sys}$=98 K,
antenna temperature T_{ant}=72 K,
receiver temperature T_{rec}=18 K,
effective area S_e = 3400 m^2.

The antenna temperature T_{ant} can be decreased 1.5-2 times after the modernization of the main circular reflector.

Fig.14. *The location of the receiver horn of the zenith observation cabin.*

BASIC DATA REDUCTION PRINCIPLES

Two types of problems can be posed and solved using the radiometer described abo
ve:

1) search for objects and measurement of their parameters;

2) synthesis of one- and two-dimensional image of a source.

A common case of solving the two problems is described by Fridman (1985) and i
represented with a block-diagram (Fig. 15).

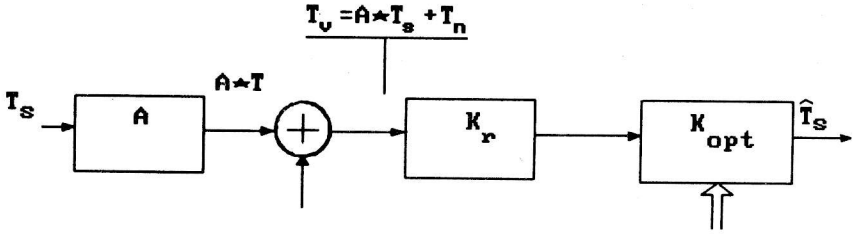

Fig.15. *The block-diagram illustrating a common case of search for objects and synthesis imaging of radio sources.*

Two-dimensional source brightness temperature distribution $T_s(x,y)$ is smoothed by the beam pattern $A(x,y)$ of a radio telescope. This smoothed signal is distorted by the additive noise T_n. The first step of data reduction is low-frequency filtering with the amplitude frequency response characteristics of a rectangular shape, with the cut off at the boundary spatial antenna frequency U_b. All spatial harmonics with such filtering pass through with the same weight, while the noise component U_b is excluded. The further data reduction consists in transformation of observational data

$$T_v = A * T_s + T_n$$

with the aim of extracting the information on T_s defined by the observer.

The signal/noise (peak signal to standard noise) ratio must be maximized at the output of the data processing system in the search for faint sources for the first problem solution. In this case we get an algorithm of coordinated filtering (correlation data reduction) with a known BP. The transfer characteristics of the optimum filtering in this case are

$$K_{opt} = K_0 \frac{\tilde{A}^*}{\Phi_n}, \qquad (5)$$

where $A(u,v)$ is the spectral characteristic of the antenna, and $\Phi_n(u,v)$ is the noise spectral density.

In the second case, when the minimum rms error criterion is used and the distribution probability is normal, the data reduction consists in linear filtering of the mixture of signal and noise by a filter with the transfer characteristic (Bracewell, 1958):

$$K_{opt} = \frac{\tilde{A}\,\Phi_s}{|\tilde{A}^*|\Phi_s + \Phi_n}, \qquad (6)$$

where $A(u,v)$ is the spectral characteristic of the antenna, $\Phi_s(u,v)$ is the energy spatial spectrum of a source, and $\Phi_n(u,v)$ is the spectral density of the additive noise.

The second problem is one of image restoration. It can be solved by either the standard methods with the *CLEAN* algorithm (Hogbom, 1974) or by the maximum enthropy method. Modifications of these algorithms and their comparison are described in suf-

ficient details in the paper by Cornwell and Braun (1989).

According to the tasks just described two runs of observations were carried out the RATAN-600. The first was carried out in 1986 with the aim of synthesizing ra images of the radio galaxies Perceus-A (3C84) and Cignus-A. The coordinate accura of synthesis imaging at the RATAN-600 was estimated from 3C84 observation. The s cond run was conducted in 1988 and was intended for the search for radio sources the two-dimensional sky survey in the narrow region of declinations (width of reg was 1′).

MAPPING OF RADIO SOURCES CYGNUS-A AND PERSEUS-A

Trial observations were carried out at the RATAN-600 in the Zenith mode in Janu ry-April, 1986, aimed at receiving of the RATAN-600 real beam pattern when operati with the ring aperture, from the radio source 3C84, as well as image synthesis of th radio galaxy Cygnus-A. Later an attempt was made to estimate the coordinate accura from the right ascention (RA) and declination (Dec) in observations of 3C84.

Real beam pattern and imaging coordinate accuracy

The source 3C84 was used for real beam synthesis. 32 scans with a step of 10 arc sec were made. 11 cross-sections across the main lobe were observed. Instability i the setting of elements (individual groups of panels fell off) played an essentia role during observations. However, the tuning-up of the system for setting the panel has considerably improved the pointing accuracy of the antenna. The results of esti- mations of the position of the beam pattern main lobe in RA after the improvements t the system of setting the elements are given in Table 3. These results were obtaine in the real observations.

Table 3.

date	α_{calc}	α_{obs}	$\Delta\alpha$, s	$\Delta\alpha-\alpha_{rms}$, s
	h m s	h m s		
03/2	3 18 52.117	3 18 53.92	1.803	0.026
05/2	3 18 52.095	3 18 53.91	1.815	0.038
06/2	3 18 52.085	3 18 53.92	1.835	0.058
11/3	3 18 51.389	3 18 53.13	1.741	-0.036
21/3	3 18 51.224	3 18 53.04	1.816	0.039
21/3	3 18 51.060	3 18 52.71	1.650	-0.127

The mean value of $\Delta\alpha$ (systematic error produced by the incorrect orientation of the electric axis) was 1.777 s, the random error $(\Sigma(\Delta\alpha-\alpha_i)^2/(n-1))^{1/2}$ was 0.07 s or 0.78″.

The estimation of the error in declination is more complicated. When we estimate

the pointing accuracy in RA we use all cross-sections of the main lobe despite the different shifts (1-4″) because the position of the maximum is stable enough. However for estimation of the pointing accuracy in declination we have to be sure that the observation cabin is exactly in the focus of the mirror. 3 cross-sections of the main lobe (exactly in the focus) and 4 cross-sections with a shift of 10″ have been used to estimate the pointing accuracy in declination. These data are given in Table 4.

Table 4.

date	shift by declinat.,″	ampl., K	halfwidth, ″
29/1	0	42.939	21.541
03/2	0	42.296	22.392
05/2	10	21.187	18.488
06/2	10	22.450	19.476
11/3	10	20.074	18.530
21/3	0	47.621	21.732
04/4	10	21.834	19.176

The pointing accuracy can be estimated from variations of the halfwidth of the BP cross-section and amplitude of an object. The value of the relative amplitude is 1±0.066 (absolute average amplitude value = 44.285 K), and the half power width of the central cross-section is 21.89″±0.36″. Then the estimate of the pointing accuracy (or the value of variation of the shift from the focus in case the antenna is pointed at the centre of the source) is 3.5″ from the amplitude variation and 4″ from the halfwidth variation. If we take the shifted cross-section (10″ from the source centre), then the relative amplitude value after division by the average source temperature in the centre is 0.48±0.02, and the value of the half power width of this cross-section is 18.92″±0.42. Then the estimate of the pointing accuracy for the cross-sections with the shift of 10″ from the centre is 0.3″ from the amplitude variation and 1.5″ from the half power width variation. The large value of error when pointing to the centre of an object can be explained by the instability of antenna setting at the beginning of observations and also by the fact that small variations of the halfwidth and amplitude values associated with the data processing quality (e.g., Gauss-analysis) may correspond to sufficiently large shifts (>3″) from the focus for the Bessel beam pattern. The accuracy of antenna setting estimated from the shifted cross-section can be readily explained by the accuracy of setting the observation cabin in the focus of the radio telescope since the temperature variations over 3 months (length of the observational run) may change the cabin position by 2-3 mm. This value corresponds to a change in declination by 1-1.5″ for the elevation of 3C84 (the shift of the observation cabin by 1 mm corresponds to a change of 0.385″ in elevation).

It is interesting to estimate the accuracy of the antenna pointing to an object from a single transit of the reference source NGC 7027 in the experiment "Zenith-88" (see below). The half power width of the BP, accounting for the size of an object

(5″), differs from the calculated BP by 0.09″. It can be explained, of course, the error in measuring the half power beam width since the step of recording is eq to 1.11″. But if this error is considered as a result of the erroneous pointing, value 0.09″ of the halfwidth variation corresponds to the shift of the beam from object centre by a value ≤1.5″, i.e. it is in the limits of the accuracy of the ca setting.

So, in actual fact, the accuracy of antenna pointing to a source in elevation declination) is defined completely by the accuracy of observation cabin setting, it is varied in the limit up to values ≤1.5″ in the observations carried out.

The "dirty" 3-dimensional profile of the radio source 3C84 (actually the real of the RATAN-600 in the Zenith mode) observed in 1986 is shown in Fig.16.

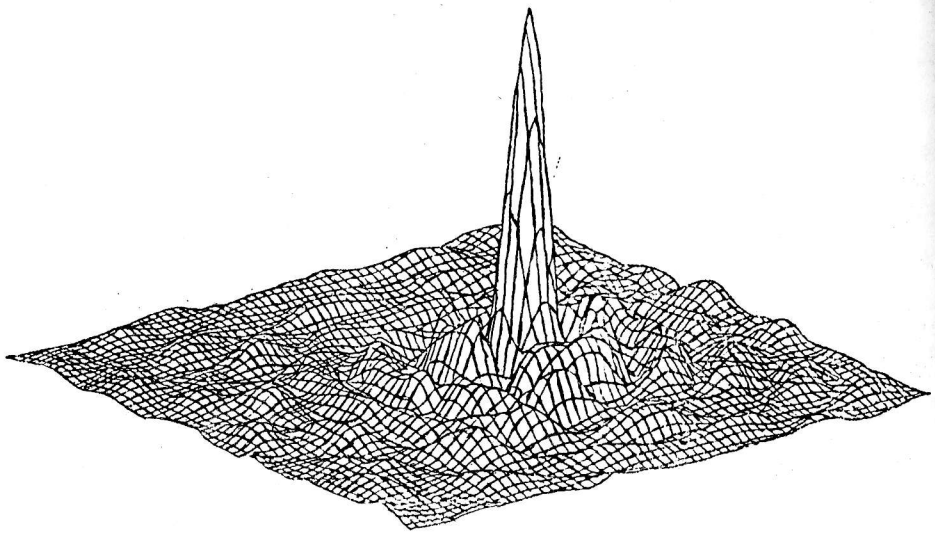

Fig.16. *A three-dimensional profile of the radio galaxy Perseus-A (3C84).*

Image synthesis of the radio source Cygnus-A

Observations of the radio galaxy Cygnus-A were carried out parallel to the radi source 3C84. 32 scans have been made with a 10″ step with several cross-sections fo each shift. The best cross-sections were selected by the lowest noise criterion. Af ter that the linear background (baseline) was subtracted. Then the cross-sections we re grouped into a two-dimensional array with a step of 5″ in both dimensions. The la cking cross-sections have been calculated by the Newton interpolation method in co lumns. The dirty image of the radio galaxy Cygnus-A observed in the near-zenith synt hesis mode is shown in Fig. 17.

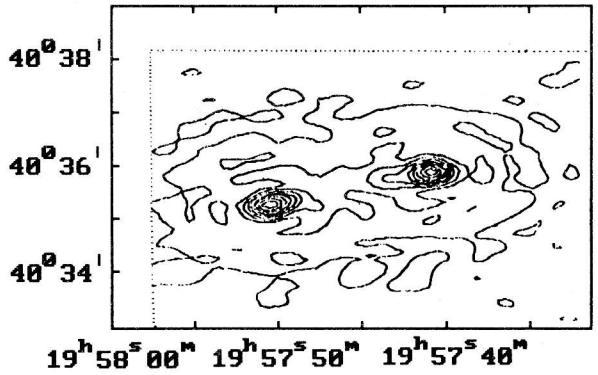

Fig.17. *Isolines of a "dirty" image of the radio galaxy Cygnus-A.*

Data reduction

Restoration of the image was performed in two ways:

a) with the Wiener filter (see formula 6);

b) by the *CLEAN* method.

Calculated and synthesized beam patterns were used for the restoration. The results of restoration with both beam types are practically the same. The results of the image restoration for the radio galaxy Cygnus A for both beam types and the present map of this source are given in Fig. 18.

A higher quality result (superresolution) can probably be obtained with the use of modern powerful methods of restoration (Terebizh, 1990).

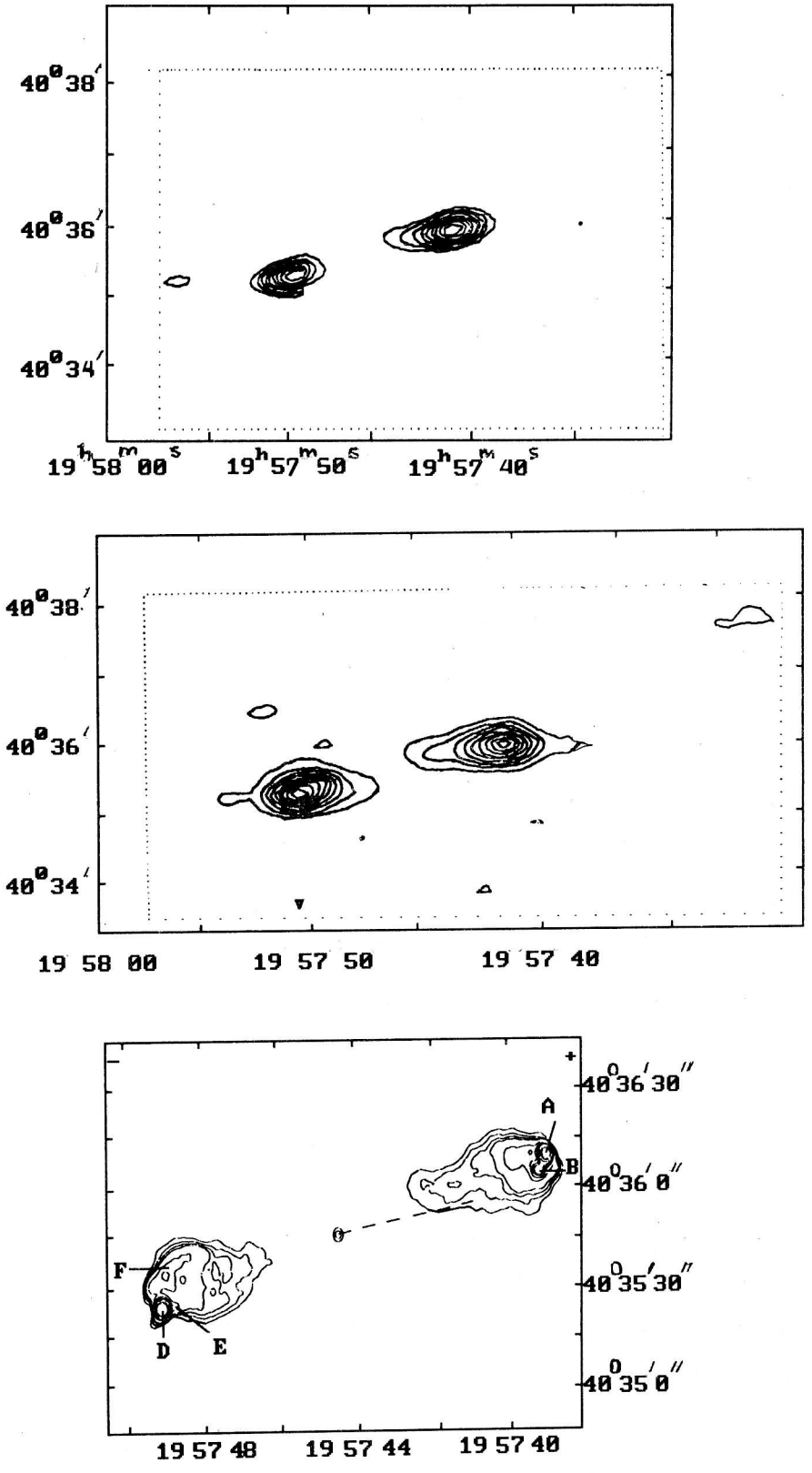

Fig. 18. a) *Isolines of the "cleaned" (with the Wiener filter) image of Cygnus-A.*

b) *Isolines of the CLEANed image of Cygnus-A.*

c) *A contemporary map of the radio galaxy Cygnus-A obtained at 6 GHz (Alexander, 1984). The dashed line shows the jet line observed by Perley (1984).*

Observations

A survey in the Zenith mode was carried out in 1988 at the 8.0 cm wavelength (Mir galiev et al., 1991).

Calibration of the survey was made by the source NGC 7027. The flux density of this source is 4.45 Jy at 8.0 cm on the scale of Baars et al. (1977). The antenn temperature of the source was 5.22 K. The effective area at this wavelength S_e wa 3400 m^2. The record of NGC 7027 transit across the beam of the RATAN-600 is shown i Fig. 19.

The survey was carried out in a range of right ascentions (RA) of 8^h - 14^h and declinations of $47^\circ 6' 45'' - 47^\circ 7' 45''$, i.e. in an area of 1.02 square degrees. 5 cross-sections with a step of 15″ were made, 5-7 observations for each cross-section. The integration time was 0.3 s. The dispersion of records after averaging but before smoothing was 3.5-4 mK.

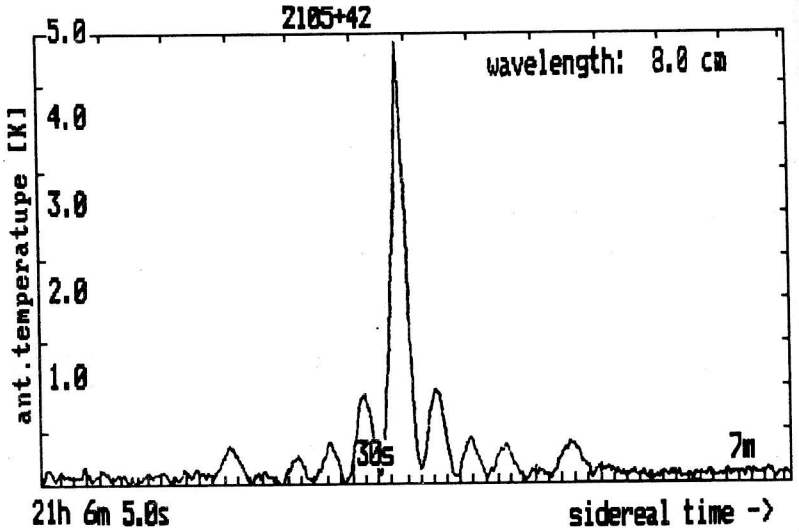

Fig. 19. *The curve of transit of the radio source NGC 7027 across the BP.*

Data reduction

Two independent methods were used in the data processing. The first consisted of Gauss-analysis of half-sums and half-differences of several records at each cross-section. Preliminarily the records were divided into two groups and averaged by ordinary addition of observations over several days at each cross-section. After that we made Gauss fitting (in the manner described in the paper by Ivanov (1979) of half-sums and half-differences of these groups. We considered sources stronger than 3σ. A source was considered if it was present in the half-sums and absent in the half-differences.

The second method consisted of two-dimensional data reduction of initial recordings with the application of robust averaging algorithms (i.e. resistant to the influence of anomalous elements of a sample). We used the Hodges-Lehmann procedure

(Erukhimov et al., 1990) for the robust averaging of recordings over several days. After that recordings were unified into two-dimensional arrays and for convenience were divided into half-hour areas along RA, i.e. 12 initial arrays of 6000 × 5 points were produced. The F-format (Verkhodanov et al., 1993) similar in its characteristics to the FITS format (Wells et al., 1981) was used for storage on a hard disk. The next step was convolution of data with the point spread function (beam) curve to improve the signal/noise ratio, i.e. signal optimum filtering:

$$S = \frac{Q * A}{A^2} \qquad (7)$$

where Q is the two-dimensional matrix of observations, $A(\theta)=J_0^2(\pi D\theta/\lambda)$ is the two-dimensional beam pattern, and S is the resulting array of convolution.

After that each file was divided into areas with a length of ≅8-10 patterns on the abscissa axis (RA) with the two beam patterns overlap. The size of this area is defined by the raised zero level after convolution of the beam pattern with itself. We supposed that there were sources in the area if the dispersion of this area, σ_0, was 1.5 times greater than the dispersion of the two-dimensional half-hour recording: $\sigma_0 \geq 1.5\sigma$. To detect sources, we used *CLEAN* algorithm (Hogbom, 1974). After detection of a maximum in the area (maximum is considered as a source if the halfwidth of a possible source $\theta_s \geq 2\theta_{0.5}$, i.e. $\theta_s \geq 2.^s9$ for abscissas and $\theta_s \geq 29.9''$ for ordinates) the function Z equal to $Z=A*A/A^2$, i.e. convolution of the BP with itself, was subtracted in the maximum position from the dirty image. The function Z was subtracted with the loop gain 0.4. After that the next source with the amplitude $S_s>3\sigma$ was searched for in the area explored. This iteration was continued until all sources with an amplitude larger than 3σ were detected. In case the sources of such an amplitude were absent the iteration in the next area was started. All the desired sources were assumed point-like.

To check the reality of the detected sources, initial recordings were divided into two groups for the robust averaging in each group. After that the difference was calculated. The described method was applied to these two groups. An analysis of the differences confirmed steady detection of sources in robust sums.

After comparing results of the two types of data reduction a resulting catalogue was issued.

Specification of source coordinates was performed, with slight modifications, in the manner described in the paper of Bursov et al. (1989). The method is based on the two-dimensional convolution with the point spread function. Since the convolution is an integral with infinite bounds, while our data are limited, we used the "weighted convolution" to specify positions of sources:

$$S_{ij} = \frac{1}{m_{ij} n_{ij}} \sum_{k}^{m_{ij}} \sum_{l}^{n_{ij}} Q_{kl} A_{k-i,l-j}\,, \qquad (8)$$

where Q, A are the arrays described earlier, m_{ij}, n_{ij} are the boundaries of the cros sing of matrices in the convolution, i.e. a number of pair multiplications in the su at the current step of the convolution. The search for the true maximum was performe by inscribing the parabola into the region near the maximum value of the convolutio curve. The position of the true maximum was detected by the parabola parameters.

The coordinate definition accuracy of this manner was $0^s.1$ in RA and 2″ in decline tion. The accuracy of the flux density definition after comparing the two manners o the search for sources was about 10% for sources of 40 mJy and stronger, about 20 for sources of 20-40 mJy, and about 40% for the sources fainter than 20 mJy.

Results

The main result of this work is the catalogue of 70 radio sources published in th paper of Mingaliev et al. (1991).

This was the first catalogue in this region at the wavelength 8.0 cm with th depth up to 15 mJy.

We have made the first attempts at identifying the detected sources with th Dixon's catalogue "MASTER.LIST" (version R42), the catalogue of Condon et al. (198 with the objects detected on the VLA at 1.4 GHz, and also the optical catalogues o the QSOs (Hewitt & Burbidge, 1987; 1989). No identifications have been found. Th catalogue "MASTER.LIST" of version R42 and optical catalogues have no sources in th region of our survey. The catalogue of Condon et al. (1989) crosses our region in th range from 9^h30^m to 10^h. The sources from our survey are absent in the zones of VL observations, and the sources of the catalogue of Condon et al. (1989) have the flu densities in this region fainter than 10 mJy. Therefore the sources of our catalogu have not been identified with the objects of the used catalogues.

The three strongest sources (rz5, rz9, rz55) of our survey have been identifie with the sources from the recently published catalogue (Gregory, Condon, 1990) obser ved in Green Bank at 4.85 GHz. Our coordinates of these sources for the epoch 1950. and their flux densities are

rz 5	8:20:15.2±0.1	47:01:37±2	55±6
rz 9	8:38:13.2±0.1	47:03:34±2	44±6
rz 55	13:10:08.4±0.1	47:07:00±2	35±6

The coordinates of the corresponding sources in the catalogue of Gregory and Condo (1990) and their flux densities are

8:20:14.8±1.1	47:01:38±12	73±9
8:38:13.8±1.5	47:04:07±17	37±6
13:10:05.4±1.6	47:07:13±22	42±7

The difference in coordinates of the source rz9 can be explained by the possible e tention of this source.

One of the useful results of the data reduction for producing this catalogue was the creation of a flexible astronomical data processing system at the RATAN-600 for IBM PC/AT-386 in the UNIX operating system (Verkhodanov et al., 1992).

The additional data reduction of this survey was performed recently. Some continuum spectra of sources and optical identifications with the Palomar Sky Survey objects were obtained (Verkhodanov, 1993). In particular, we can say that some detected sources have been identified with the objects of the Dixon's catalogue "MASTER.-LIST" of version R43 and UTRAO catalogue at 365 MHz which was kindly made available to us by Dr. H. Andernach.

FINAL ANALYSIS

The most important results of the operation of the zenith observation cabin are the introduction into the standard mode of the adjustment of the RATAN-600 with the circular aperture, evaluation of the synthesis imaging of the radio galaxy Cygnus-A, and the two-dimensional sky survey resulting in the catalogue of radio sources.

One of the results of the observations carried out at the RATAN-600 is a conclusion about the advantages of the Zenith mode of work "by-lists" (it means observations of individual sources in the near-zenith zone) before the deep sky surveys in this mode.

Let us consider this variant of operation of the RATAN-600 in more detail.

Assume that the effective area of the radio telescope is about 4000 m^2, and the receiver noise is about 4.5 mK, which corresponds to 3 mJy. Then, considering sources stronger than 3σ (i.e. about 10 mJy and more) in the initial recording as real sources, we can obtain an expected number of radio sources in the near-zenith region. Using Green Bank survey data (Becker et al., 1991) at the frequency close to that of our receiver (5.85 GHz), we can obtained a rough number of objects in this zone. The size of our sky area ($\pm 4.5^\circ$ from the Zenith at the latitude of the RATAN-600 or in a strip of $39^\circ 20' - 48^\circ 20'$ in declination) is equal to about 2337 square degrees, approximately $3 \cdot 10^{10}$ $arcsec^2$. The number of sources in this zone from the *log N - log S* curve (the same paper) is approximately $2.2 \cdot 10^4$. Then assuming that their size is about the BP size we can estimate the ratio of the area occupied the sources with flux densities greater than 10 mJy to the area of the possible zone of observations in the Zenith mode:

$$\frac{S_{sour}}{S_{sq}} = 3 \cdot 10^{-4}$$

The time needed for observation of the whole area with a step of 15″ (a little less than the size of the BP) will be 5.9 years in the case of a single transit at each

scan. Of course, such surveys are very important in the case of exploration of t population of sources from 10 (or even 1 mJy) to 50-60 mJy. However, the informatio obtained will be less significant because it will halt other (may be more important programs at the RATAN-600, because the simultaneous operation of the RATAN-600 in th Zenith and other modes is impossible.

The ratio S_{sour}/S_{sq} shows the efficiency of the telescope in relation to obtainin meaningful information. Investigation of background radiations on scales severa times the BP size, or noises in the absence of a signal, are also interesting an provide useful information. Thus, in general the value $3 \cdot 10^{-4}$ is slightly underesti mated, although it reflects the real situation.

To get out of this difficulty, it would be better to observe separate regions o the sky which have interesting objects. These regions may have either several object or one object (see "Astrophysical tasks for the observation cabin No. 6"). Having list of such areas, a user (observer) can use more effectively the telescope tim both from the view-point of parallel programs and storing and processing of inform ation. Another important feature in the work "by-lists", as shown earlier, is th possibility of the long-term accumulation of signals in the tracking mode for eac radio source from the list. For example, we can improve by almost 5 times the sensi tivity for the current receiver at 8.0 cm when tracking an object by moving th carriage. This improvement corresponds to a sensitivity of recording of about 1 mJy Therefore the future sky surveys at the RATAN-600 in the Zenith mode will be asso ciated with the work "by-lists".

In this chapter we can also estimate the informativity (i.e. information through put in binary units per unit of time) of the telescope RATAN-600 in the Zenith mode

The information throughput of the radio telescope in this case is the amount o information I read from unit solid angle. Let us use the formula derived by Korolkov and Fridman (1970) with the Shennon's method (Shennon, 1963) for calculation of th informativity I:

$$I = 2 \frac{D_x D_y}{\lambda^2} \log_2 \left[1 + \left(\frac{S_e}{D_x D_y} \sqrt{\frac{D_y}{\omega\lambda}} \frac{\tilde{T}_\lambda}{\Delta T_0} \right)^2 \right]. \qquad (9$$

Here S_e is the effective collecting surface of the radio telescope, D_x, D_y are th maximum linear sizes of the system, λ is the wavelength, ΔT_0 is the fluctuation sen sitivity of the radiometer with the integration time $\tau = 1$ s (after n averagings), $\tilde{T}_\lambda$ is the spatial spectral density of the sky brightness temperature at the wavelengt λ, and ω is the angular velocity of the Earth rotation ($\omega = 0.72 \cdot 10^{-4}$ rad/sec). I our case $D_x = D_y = R = 576$ m. The dependence $\tilde{T}(\lambda)$ is taken from the paper of Korolkov and Fridman (1970). Let us estimate the informativity of the telescope for 3 waves - 8, 2.7 and 21 cm. At the wavelength 8 cm $\tilde{T}_\lambda \cong 10^{-5}$K (Fig. 20), at the wavelength 2.7 cm

$\tilde{T}_\lambda \cong 5\cdot 10^{-7}$, and at the wavelength 21 cm $\tilde{T}_\lambda \cong 5\cdot 10^{-4}$. Let the effective area be equal to 3500 m^2. The results of calculations for different sensitivities are given in Table 5.

Table 5.

ΔT_0	7mK	3mK	1mK
λ, cm		I, bit/sr	
2.7	$1.2\cdot 10^9$	$1.6\cdot 10^9$	$2.1\cdot 10^9$
8	$2.4\cdot 10^8$	$2.8\cdot 10^8$	$3.6\cdot 10^8$
21	$4.7\cdot 10^7$	$5.5\cdot 10^7$	$6.7\cdot 10^7$

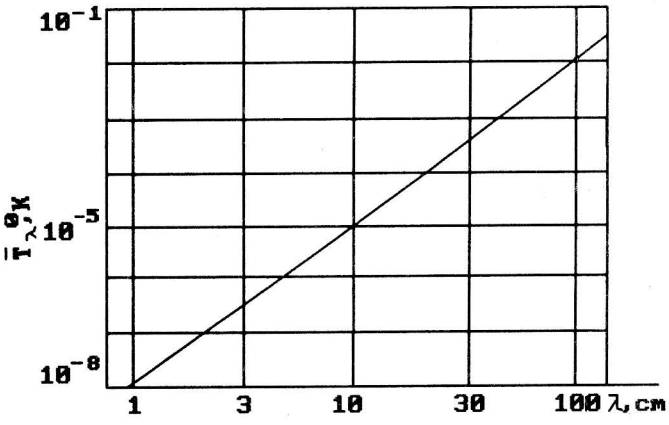

Fig.20. *The dependence of the spatial spectral density of the sky temperature on the wavelength.*

The total amount of information obtained in the survey of 1988 (5 cross-sections × 5 transits for each cross-section × 6 hours × 2 × 6000 points in each half-hour recording × 16 bits per pixel) is $2.9\cdot 10^6$ bit for an area of 1.02 square degrees and sensitivity of ≅ 4mK. If we take into account that in our survey the element of resolution corresponds to 10 pixels and that, roughly, 1 element of resolution carries one bit of information, then the informativity of our survey is $9\cdot 10^9$ bit/sr, which is greater than the calculated informativity by a factor of about 1.5. However, with allowance made for the estimate of the possible number of sources the amount of useful information will be tens of times less.

As is clear from the given estimates of the informativity, the first survey at the RATAN-600 realized potential informative antenna capabilities, conditioned by the antenna geometry at the wavelength 8.0 cm.

We have considered the formal potential informativity of the RATAN-600 in the Zenith mode. However, it can never be realized in practice due to the small field of view in this mode. E.g., it is possible that during a given day no source falls within the RATAN-600 BP in the mm wavelength range with a resolution of about 1″ in the transit mode. Therefore it is important to investigate all the possibilities of increasing the flow of information dI/dt. Multibeam observations (see below) are one of the variants of solution to the problem. In the ideal case one may increase the efficiency by a factor of $S_{geom}/H\lambda$ times, where $S_{geom}=2\pi RH/\sqrt{2}$, H is the height of an element, and R is the radius of the RATAN-600.

1. Radioheliograph

One of the interesting operational modes using the main and the conical secondary mirrors of the radio telescope RATAN-600 is the radio heliograph mode. This mode has been described in details in the paper of Gelfreikh and Opeikina (1992).

As is known, the main mirror of the RATAN-600 consists of 900 independent elements arranged in a circle. Each of the elements can be shifted radially and tilted in elevation and azimuth. The incident wave reflected from the main mirror is "picked up" in the focus of the secondary mirror. The latter can run inside the circle along the radial and arc rail-tracks. Such mobility of all antenna elements makes it possible to realize many telescope operational modes, which, in turn, allows us to choose the optimum method for solving the observational task.

The radioheliograph mode may provide the best resolution for two-dimensional mapping of the Sun.

In this mode a minimum number of conditions imposed on the shifts of the antenna, when forming its reflecting surface, gives a maximum aperture. All elements able to redirect solar rays to a desired focal point form the antenna surface. Calculations show that to observe a source with an elevation of 60° it is possible to set more than 2/3 of antenna elements. The corresponding aperture has the size of 600m × 400m.

2. RATAN-600 as a phased feed array

Being the largest (relative to D/λ performance) reflector antenna, the RATAN-600 radio telescope yet has specific difficulties of parabolic antennas connected, first of all, with their small field of view (that depends on $(D/\lambda)^2$), which is $\sim 6.8 \cdot 10^{-11}$ sr for the wavelength of 8 cm.

There are several methods for eliminating this shortcoming in the Zenith observational mode at the RATAN-600:

1) The use of a feed array to exclude aberrations (Pinchuk et al., 1989). In this case the installation of a phased feed array over the focal region of the RATAN-600 ring aperture would allow us:

- to increase considerably the sky region, that could be synthesized in the Zenith observational mode;
- to realize a long-time tracking of extended sources after updating the telescope remote control peripherical equipment;
- to realize all modern methods of closure of amplitudes and phases in the interferometric mode and considerably increase the telescope dynamic range.

As a result, about 3 steradian of the celestial sphere can be investigated with a sensitivity close to that of the VLA in D-configuration (Thomson et al., 1980). Seve-

ral possible versions of hybrid mirror antennas (HMA) in the mode of entire ring aperture are presented in Pinchuk et al., (1989) (see Fig. 21).

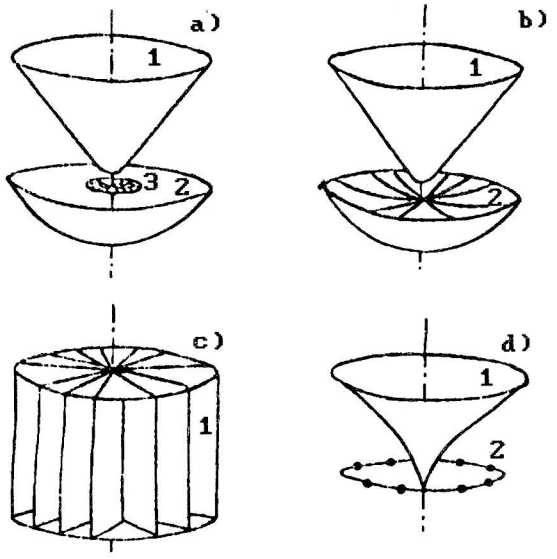

Fig. 21. *Variants of the up-dating of the secondary mirror in the HMA operation with the complete circular aperture:*
a) *1 - the conic reflector, 2 - the parabolic mirror, 3 - the flat array of the pimary feeds;*
b) *1 - the conic reflector, 2 - the horn-parabolic antennae;*
c) *1 - the horn-parabolic antennae;*
d) *1 - the non-symmetrical circular parabolic reflector, 2 - the circular array of the primary feeds.*

2) To divide the main surface by N ring surfaces with different eccentricities but with a common focus. This allows the formation of N beams but with a loss of effective area in each direction by N^2 times (Babushkina & Fridman, 1985). In this case we have a set of $J_k(x)$. This set permits the possibility of synthesizing a beam of a desired shape using corresponding weights t_k for the components:

$$F(x) = \sum_{0}^{N} t_k \, J_k(x) \qquad (10)$$

In particular, an "optimum" power beam pattern $J_1(x)/x$ with a uniform spatial frequency response characteristic can be shaped. A similar variant has been developed at the Coolgura Observatory (Australia) at a radio telescope specifically designed for solar activity investigation at the 3 m wavelength (Wild, 1969). This type of observation was called J^2-synthesis by Wild (see also Esepkina et al., 1973).

3) Following Fizeau's pioneering works to divide the main aperture into separate synphase elements and to obtain simultaneously and without loss several non-distorted images by the method of amplitude-phase masks.

If one is restricted by the interference of a cylindrical wave reflected from the secondary mirror with the azimuth component of the field, then the RATAN-600 can be converted with a 1000-elements matrix radiometer into a 1000-elements phase array with a limiting field of view $\sim(\lambda/d)^2$, where d is the size of an element of the RATAN-600, i.e. the field of view is $(D/d)^2$ times larger than in the ordinary mode. Formally the number of elements could be S_{geom}/S_{Fres}, where S_{geom} is the total geometrical area of the RATAN-600 ring aperture, and S_{Fres} is the area of the Fresnel

spot:

$$S_{Fres} = \lambda R, \qquad (11)$$

where λ is the wavelength, and R is the radius of the RATAN-600. While at long waves $S_{Fres} \sim d^2$, in the millimetre range one element may contain more than 10 Fresnel zones and the field of view will be equal to λ^2/S_{Fres} or about 10000 patterns. Rapid progress in the creation of matrix radiometers and the practically unlimited expansion of the computer facilities permits us to hope that in the next century this variant will be realized.

Comparison with the millimetre array of the USA

As is known, the efficiency of Y-like and ring-like configurations of N antennas is different (Hjellming, 1989). Detailed estimations in NRAO led to the project of the millimetre array, consisting of 21 antennas randomly placed in a circle (Fig.22). In case of implementation of the limiting variant of conversion of the 900-elements RATAN-600 into a controlled phase array, this array may be considered as 8 NRAO projects enclosed in each other. This will permit either an increasing the potential of one subarray of 8 times or realization of the mosaic mode of imaging large areas. Arranging all beams along the meridian we can achieve a large dayly field of view. This field will be sufficient for mapping radio galaxies in the millimetre range, and in the decimetre range for surveying the whole sky accessible to the Zenith mode during one day.

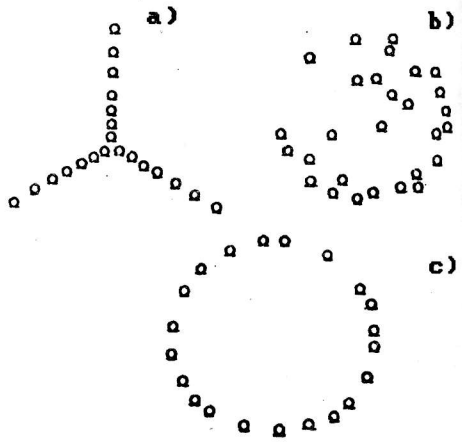

Fig.22. *Antenna distributions corresponding to:*
a) *a VLA-like three-armed radial distribution of 21 antennae;*
b) *a non-redundant 2-dimensional array with antennae at random locations, analogous to a "crystalline" array design; and*
c) *a circular array with antennae at random locations (Hjellming, 1989).*

In Table 6 are listed the principal quantitative parameters of three arrays of the NRAO project for observations of radio sources at a declination of 60°, assuming a bandwidth of 1 GHz, system temperature of 200 K for 2-min snapshots and an 8-hour tracking in Zenith for the wavelength 3 mm (Hjellming, 1989). Here N is the number of antennas, D is the diameter of the antenna, B is the size of the antenna array, N_{occ} is the number of occupied cells on the UV-plane, f_{occ} is the fraction of the occupied cells ($f_{occ}=N_{occ}/N_{occ,max}$), $N_{occ,max}$ is the maximum number of cells on the UV-plane, θ_{beam} is the resolution of the array, S is the rms sidelobe level, σ is the

rms point source sensitivity, and ΔT_b is the rms brightness temperature. Index *na* means natural weighting and *un* means uniform weighting.

Table 6. **Parameters for 3 arrays with N=21, D=10 m**

Congfiguration	3 radial arms (Y-configuration)		Randomised circle		Filled circle	
B (metres)	300		300		90	
D (metres)	10		10		10	
$2B/D$	60		60		18	
Observation time	8h	2m	8h	2m	8h	2m
N_{occ}	2804	362	3418	410	308	204
f_{occ}	0.708	0.091	0.863	0.104	0.890	0.589
S_{na}	0.0325	0.0565	0.0200	0.0499	0.0717	0.0798
S_{un}	0.0189	0.0526	0.0171	0.0494	0.0570	0.0700
$\theta_{beam,na}/\lambda$(mm)	1.30″	1.20″	0.51″	0.49″	2.09″	1.99″
$\theta_{beam,un}/\lambda$(mm)	0.54″	0.82″	0.48″	0.49″	1.53″	1.75″
σ_{na} (mJy)	0.079	1.22	0.079	1.22	0.079	1.22
σ_{un} (mJy)	0.154	1.28	0.096	1.23	0.187	1.40
$\Delta T_{b,na}$ (mK)	0.64	11.5	4.07	69.1	0.2	4.2
$\Delta T_{b,un}$ (mK)	7.08	25.8	5.62	68.8	0.46	6.2

The distinguishing feature of the RATAN-600 operation in this mode is exceptional flexibility. Introducing a concept of "virtual radio telescope" (or virtual two-element radio telescope), we can bring into agreement the spatial frequency response characteristic of an object and antenna, and control the trajectory of a pixel on the *UV*-plane in tracing (instead of fixed ellipses in ordinary systems). "Mosaic" methods are used for the imaging of extended objects. These methods demand optimization of the parameter ND instead of $N\pi D^2/4$, where N is the number of antennas, and D is the diameter of the mirror (Cornwell, 1989). The RATAN-600 allows us to change the ratio between N and D_e over sufficiently wide limits.

Although we mainly concern ourselves here with the problems of the Zenith synthesis, transition to the phase and amplitude controlled aperture synthesis allows us, with the (reconstructed) type *VI* observation cabin, to trace objects from rise to set with the aperture limited only by the possibilities of angular displacements in azimuth.

Rejecting the discrete character of observations in azimuth, we improve UV-plane filling when realizing the project variant of azimuth aperture synthesis (see e.g. Minchenko, 1977; 1978).

Let us compare parameters of the RATAN-600 in the millimetre array mode with the variant of the $100 million USA project. Let the system temperature be 200 K and 100 K, bandwidth 1% (1 GHz) and 10% (0.1 GHz), and tracking 2 min and 1 hr. The calcula-

ted parameters are given in Table 7. For more details about this mode of operati see the paper of Parijskij and Verkhodanov (1993).

Table 7.

Configuration	Random antenna positions on the circle			
B (metres)	600			
D (metres)	10			
$2B/D$	120			
S_{geom} (m^2)	1650			
T_{sys}	200 K		100 K	
$\Delta f/f$	1%		10%	
Observation time	1h	2m	1h	2m
N_{occ}	1965	437	1965	437
f_{occ}	0.188	0.042	0.188	0.042
S_{na}	0.0242	0.0478	0.0242	0.0478
S_{un}	0.0226	0.0478	0.0226	0.0478
$\theta_{beam,na}/\lambda$(mm)	0.18″	0.23	0.18	0.23
$\theta_{beam,un}/\lambda$(mm)	0.19″	0.23	0.19	0.23
σ_{na} (mJy)	0.24	0.94	0.039	0.21
σ_{un} (mJy)	0.25	0.95	0.040	0.21
$\Delta T_{b,na}$ (mK)	9.09	35.8	1.48	7.96
$\Delta T_{b,un}$ (mK)	9.47	35.9	1.52	7.96

On the problems of object tracking

As is noted above, the future performance of the RATAN-600 in the Zenith mode l associated with work by-lists, in which object tracking mode can be realized. Let u consider this mode in more detail (see also (Verkhodanov, 1993a)).

There are several types of tracing which can be implemented in operation with ob servation cabins of the type *I-VI*. Some of them are

1) tracking with the help of moving the carriage;

2) tracking in a "relay-race" manner;

3) tracking of objects (Sun) with cabin *III* moving along the arc rails in th Southern sector of the RATAN-600.

The first manner will be discussed below.

The second manner, worked out and used by O.A.Golubchina (Golubchina & Golubchin 1981; 1983) for solar investigations, provides a possibility for tracing objects b transpositions of individual groups of elements while the object under study is i the field of view of the radio telescope. It is clear that this method is adequat only for strong radio sources because of the small antenna area.

The third manner has not been practically tested yet, though it may play a very important role in Solar activity exploration after modernization of the railway.

In the Zenith mode 2 manners of object tracing can be used:

1) tracking by moving the carriage;

2) tracking in the "fast antenna transposition" mode.

Let us consider the first of these methods. As has been said above, in the design of the type *VI* cabin an allowance was made for tracking an object by moving the carriage. The carriage of the cabin moves in this case along the arc rails which are a part of the cabin's construction (Fig. 23). The "sliding" mode, when the carriage speed is not equal to the velocity of an object moving across the BP, and the tracking mode, when the velocities are equal, are investigated in detail in the experiment by Mingaliev (1985) for the case of a regular observation cabin. The carriage moves exactly at a right angle to the radial direction.

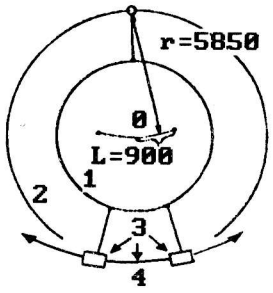

Fig.23. *A top-view schematic of the observation cabin of type VI:*
0 - the reflector focus;
1 - the conic reflector;
2 - the parabolic reflector;
3 - the mobile supporting legs (pylons);
4 - arc rails.
r, l - in mm.

One of the distinctive features of observations in the Zenith mode is that aberrations existing for lower elevations disappear in the near-zenith zone ($h > 85^\circ$) (Stotskij, 1972). On the other hand, we have to allow for the elevation correction dz arising out of the source displacement from the meridian (Fig. 24). The effect of this correction is not essential at medium elevations, but it may considerably exceed the antenna beam size in the near-zenith zone. This correction can be calculated by the formula:

$$\cos(z+dz) = \sin\varphi \sin\delta + \cos\varphi \cos\delta \cos t_h,$$

or (12)

$$dz = \arccos(\sin\varphi \sin\delta + \cos\varphi \cos\delta \cos t_h) - z.$$

Here z is the zenith distance, φ is the grid latitude (in the case of RATAN-600 $\varphi = 43.^\circ831$), δ is the declination of a source, t_h is the hour angle equal to

$$t_h = \frac{15\ l \cos\delta}{3600\ V_s}\ \text{grad}, \qquad (13)$$

l is the transversal shift of the primary feed from the focus in mm, and V_s is the

travel velocity of a source at the elevation h calculated by Trushkin's formula:

$$V_s = \frac{21.23 \cos \delta}{1 + \cos h} \text{ mm/s.} \quad (14)$$

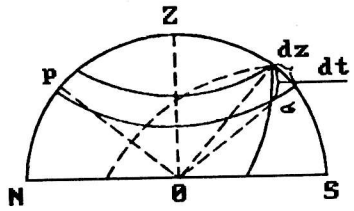

Fig.24. *The change in the zenith distance by the value dz when observing the source σ with the shift dt from the meridian.*

Account must be taken of the corrections for transversal and longitudinal shifts in the calculation of the sliding mode because the receiver is moving in a circle with the radius r=5850 mm at the time the carriage is moving along the arc rails. The value of the transversal shift is $x=r \sin \theta$, and the value of the longitudinal shift is $y=r(1-\cos \theta)$, where angle θ, the angle of the carriage displacement along the arc rails by the value l, is equal to l/r.

The difference between the velocity projection of the carriage motion onto the X-axis and the uniform velocity can be neglected, because even at maximum shifts of the horn from the focus (L=900 mm) this difference is only about 1%.

Using these formulae we simulated the recordings of source transit across the beam of the RATAN-600 in the Zenith mode with the different mismatch coefficients:

$$k = \frac{(V_{car} - V_s)}{V}, \quad (15)$$

where V_{car} is the rate of the carriage movement, and V_s is the velocity of the object motion computed by formula (14), i.e. $V_{car}=(1+k)V_s$. The coordinate of a source on the carriage at the moment t is equal to

$$l = -L + r \arcsin \frac{(t - t_{cul}) \cdot V_s}{r}, \quad (16)$$

where L=900m is the maximum shift from the focus, and t_{cul} is the time of the source culmination.

The coordinate of the horn position on the carriage at the moment t is equal to

$$l_{car} = -L + (t-t_{cul})\, V_{car} + l_0, \quad (17)$$

where l_0 is the initial horn coordinate before the carriage starts to move. Then the transversal shift in mm between the horn and the object at the moment t is

$$x = (l_{car} - l_s) \cos \theta = [kV_s(t-t_{cul})+l_0] \cos \theta \quad (18)$$

or

in arc sec $\quad X'' = 15 \frac{x}{V_s} \cos \delta,$

where $\theta = \dfrac{V_{car}(t-t_{cul})}{r} = \dfrac{1+k}{r} V_s (t-t_{cul})$. (19)

The longitudinal shift Y from the BP centre is the sum of two components. The former, Y_1, is the shift by the elevation connected with the non-meridian observations. The latter, Y_2, is the very longitudinal shift from the focus due to the carriage movement along the arc rails. These components at the moment t are equal to

$$Y_1 = \arccos(\sin\varphi \sin\delta + \cos\varphi \cos\delta \cos t_h) - z,$$

where

$$t_h'' = \frac{15r}{V_s} \sin\theta \cos\delta,$$

θ is calculated by (19);

$$y_2 = r(1-\cos\theta).$$

Here y_2 is the longitudinal horn shift from the focus in mm. To transform it into arcsec we can use two methods. The first applies the formula for calculating the distance from the imaginary focus of the RATAN-600 to the centre of the circle at the elevation h (Shivris et al., 1983):

$$f = (1-F)\{R_{max} - 445\,[1/\cos(h/2)-1]\}, \quad (20)$$

where

$$F = \frac{1 - K\cos h}{1 + \cos h},$$

$$K = 1 - \left(\frac{R_{min}}{R_{max}}\right)^2,$$

R_{min} = 288470 mm, R_{max} = 287550 mm. We can find an elevation derivative and obtain the dependence of the shift in elevation on the longitudinal shift of the cabin along the radial ways. The second method is to use the formula (Stotskij, 1972):

$$\frac{dy\,(1 + \cos h)}{R} = \frac{\cos h - \cos(h + dh)}{1 + \cos h}, \quad (21)$$

where dy is the longitudinal shift of the cabin, dh is the shift in elevation, and R is the radius of the RATAN-600. The difference in the results of the two formulae does not exceed 7%. This is sufficient to simulate transit of a source across the BP of the telescope.

Simulated curves for the wavelength 8.0 cm at an elevation of 89°50′ are shown in

Fig. 25. Bessel function (2) has been used as the beam pattern. Simulated curves have been calculated for the various mismatch coefficients. It can be seen from the figure that a source is in the focal spot zone for about 43 sec. It improves the signal/noise ratio 4.8 times (halfwidth of BP = 1.8 s) due to increase in integration time and allows us to achieve a sensitivity of about 1 mJy at the wavelength 8 cm in one transit of a source.

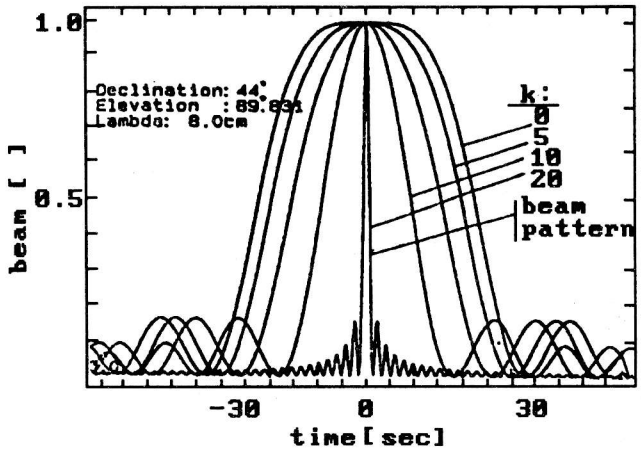

Fig.25. *The simulated curves in the "sliding" mode at an elevation of 89° 50′ for the 8.0 cm wavelength with different mismatch coefficient.*

Another interesting way of object tracking is connected with the modernization of the antenna setting system of the radio telescope. In this case we have the possibility of a fast but discrete setting of the antenna in accordance with the source motion over the celestial sphere, i.e. accumulation of the signal for the time a radio source is in the field of view of the RATAN-600 with the use of the whole ring. This time is about 1 hr. This variant may be realized at the long waves in the near future. With the employment of new generation radiometers with a sensitivity of ~1 $mK \cdot s^{1/2}$ we can attain a sensitivity of the radio telescope higher than 10 μJ per 1 hr of observations. At short waves (in the millimetre range especially) one will need to find a new precise method for setting and shifting the secondary mirror. One of the possible ways has been discussed both above and in the paper of Parijskij (1986). This method utilized the accumulated experience in automatic focus setting in the autocollimation manner with the use of part (less than 10%) of the reflecting surface, to form a controlled focal spot and standard manners of autoguiding. Introduction of the two-dimensional phased array that collects energy reflected from the entire ring in a spherical wave field of the type *VI* observation cabin allows us, at least, to follow an object from rise to set with the variable aperture dependant only on kinematic limits in displacement of elements in the angular coordinates.

Zenith mode and "three-dimensional radio astronomy"

As is shown in the papers of Parijskij & Shivris (1972) and Parijskij (1969), the distance to a pointlike source can be defined with sufficiently large antennas. This recquires fulfilment of the following condition:

$$\rho < \frac{D^2}{\lambda} \cdot \frac{S}{N}, \qquad (22)$$

where S/N is the signal/noise ratio. For the S/N=10 we have for D=600 the following table:

Table 8.

Wavelength	ρ
2.6 mm	1400 000 km
8 mm	450 000 km
2.6 cm	140 000 km
6 cm	60 000 km
21 cm	17 000 km
30 cm	12 000 km
75 cm	4 800 km

In the near field zone one can localize objects in three coordinates with the accuracy

$$\Delta x = \frac{\lambda}{D} \cdot \rho \frac{N}{S}$$

$$\Delta y = \frac{\lambda}{D} \cdot \rho \frac{N}{S} \qquad (23)$$

$$\Delta z = \frac{\lambda}{2\sin^2(D/2\rho)} \cdot \frac{N}{S} = 2\lambda \left(\frac{\rho}{D}\right)^2 \cdot \frac{N}{S}$$

Just as the two-element interferometer with the base D is the δ-filter of spatial frequencies, so the three-element interferometer with the location of elements in points 0, $D/2$, and D along the X-axis is the δ-filter of the Fourier image along the Z-axis. By analogy with the two-dimensional Bracewell formalism for the infinitely distant objects we can use the three-dimensional spatial frequency response formalism for all apertures. In this case the convolution theorem can be written as

$$T_A(x,y,z) = f(x,y,z) * \varepsilon(x,y,z), \qquad (24)$$

where T_A is the antenna temperature, $f(x,y,z)$ is the three-dimensional beam, and ε is the emissivity of an object. A ring aperture with a uniform reflection of energy has a distribution of energy in the beam described as function $(\sin az/az)^2$ in the near-field zone. Its Fourier-image is described by the triangular function in the spatial frequencies region:

$$0 < \omega < D^2/2\lambda\rho.$$

An equivalent of the curve of transit across the BP is the curve of power vari-

ation at the output of the radio telescope after its refocusing, through the introduction of the corresponding square error in the telescope aperture, a change of position of the focus, or the use of the phase distortions with the phased feed array in the focal plane. In principle, similarily to the classical phased antenna arrays or radio astronomical synthesis systems, we can divide each receiving channel by N independent ones with the different phase shifts after UHF amplifiers in the matrix radiometer. Thus we can create N independent beams to fill in the definite spatial volume around the radio telescope with the "focal spots". This volume has no maximum in Zenith (Fig.26), where it is equal to

$$V = \frac{1}{3}\pi\left(\frac{\lambda}{d}\right)^2 \cdot R_f^3 , \tag{25}$$

where d is the size of an element, and R_f is the size of the near field zone ($R_f = \sqrt{\lambda D}$). But it does have a maximum near the horizon, where

$$V = \frac{1}{3} 2\pi R_f \frac{\lambda}{d} R_f^2 . \tag{26}$$

At the centimetre waves we have in this volume about 10^{10} elements of spatial resolution with a size of

$$\left(\frac{\lambda}{D}\rho\right)^2 \cdot 2\lambda\left(\frac{\rho}{D}\right)^2 = \frac{2\lambda^3}{D^4}\rho^4 \tag{27}$$

for the space inside the radius of the geostatical orbits.

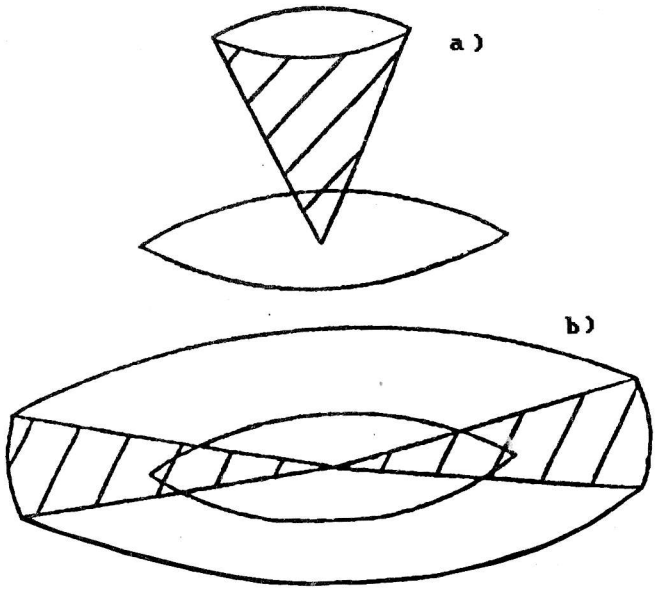

Fig.26. *The room of space around the radio telescope occupied by the focal spots when it is operated*
a) *with the circular aperture;*
b) *near the horizon.*

In this variant RATAN-600 can be used as a patrol instrument of circular survey. We do not consider "active" variants here. But the efficiency of search for the black-body objects can be easily estimated. If the size of the focal spot at the distance R is equal to S (in the near-field zone $S=(\lambda/D)^2$), then the antenna temperature will be equal to

$$T_a = T_0 \quad \text{for } S < S_{bb}$$

$$T_a = \frac{S_{bb}}{S} \cdot T_0 \quad \text{for } S > S_{bb}. \tag{28}$$

Here T_0 is the black-body temperature which we consider equal to 300 K, and S_{bb} is the area of the cross-section of the black-body emitter. In the near-field zone without focusing these expressions degenerate into

$$T_a = T_0 \quad \text{for } S_{geom} < S_{bb},$$

$$T_a = \frac{S_{bb}}{S_{geom}} T_0 \quad \text{for } S_{geom} > S_{bb}, \tag{29}$$

where S_{geom} is the geometrical area of the aperture.

Since the size of the focal spot S in the near-field zone is much smaller than S_{geom} (approaches λ^2 for $R \sim D$), then the energy gain in refocusing for the distance ρ may approach

$$G = \frac{4\pi S_{geom}}{\lambda^2}. \tag{30}$$

The authors are thankful to all the SAO collaborators who helped in the work with the Zenith mode and in the preparation of this paper.

This work was supported by the grant of the Russian Fund of Fundamental Searches No. 93-02-17238 "Radio cosmology".

REFERENCES

Afanasjev G.M., Berlin A.B.: 1984, *Radioastronomicheskaya apparatura. Thes. of the XVII All Union Conference.* Erevan. 210.

Alexander P., Brown M.T., Scott P.F.: 1984, *MNRAS*, **209**, 856.

Amstislavskij A.Z., Kopylov A.I., Prosmushkin M.I.: 1972, *Izvestiya GAO USSR AS*, L., **188**, 89.

Baars J.W.M., Genzel R., Pauliny-Toth I.I.K., Witzel A.A.: 1977, *Astron. and Astrophys.*, **61**, 99.

Babushkina S.V., Fridman P.A.: 1985, *Prepr.* No. 22L. SAO USSR AS. Leningr. branch.

Becker R.H., White R.L., Edwards A.L.: 1991, *Astropys.J.Suppl.Ser.*, **75**, 1.

Berlin A.B., Gassanov L.G., Golnev V.Ya., Lebed V.I., Nizhelskij N.A., Spangenberg E.E., Timofeeva G.N., Yaryomenko A.V.: 1982, *Radiotehnika i electronica*, **7**, 1268.

Berlin A.B., Gassanov L.G., Korolkov D.V., Lebed V.I., Yaryomenko A.V.: 1989, *Radioastronomicheskaya apparatura. Thes. of the XXI All Union Conference.* Erevan. 207.

Bracewell R.N.: 1958, *Proc. IRE*, **46**, 106.

Bursov N.N., Verkhodanov O.V., Erukhimov B.L., Lipovka N.M., Pyatunina T.B., Sobolev N.S., Temirova A.V.,Chernenkov V.N.: 1989, *Astrofiz. issled. (Izv. SAO)*, **28**, 136.

Condon J.J., Dickey J.M., Salpeter E.E.: 1989, *Astron.J.*, **99**, 1071.

Cornwell T., Braun R.: 1989, in: *Synthesis Imaging in Radio Astronomy.A Collection of Lectures from the Third NRAO Synthesis Imaging Summer School.* Eds.: R.A. Perley, F.R. Schwab, A.H. Bridle. Astron. Soc. of Pacific. 167.

Cornwell T.: 1989, in *Synthesis Imaging in Radio Astronomy. A Collection of Lectures from the Third NRAO Synthesis Imaging Summer School.* Eds.: R.A.Perley, F.R.Schwab, A.H. Bridle. Astron. Soc. of Pacific. 277.

Dibizhev A.D., Majorova E.K., Pinchuk G.A., Sinyanskij V.I., Stotskij A.A., Khaikin V.B.: 1986, *Soobshch. Spets. Astrofiz. Obs.*, **52**, 77.

Erukhimov B.L., Vitkovskij V.V., Shergin V.S.: 1990, *Prepr.* No. 50. SAO USSR AS Nizhnij Arkhyz.

Esepkina N.A., Parijskij Yu.N.: 1972, *Izvestiay GAO USSR AS,* L., **188**, 58.

Esepkina N.A., Korolkov D.V., Parijskij Yu.N.: 1973, *Radioteleskopy i radiometry* M.: Nauka.

Fridman P.A.: 1985, *Prepr.* No. 21L. SAO USSS AS. Leningr. branch.

Gelfreikh G.B., Opeikina L.V.: 1992, *Prepr.* SAO RAS , No. 96, Nizhnij Arkhys.

Golnev V.Ya., Lebed V.I., Nizhelskij N.A., Yaryomenko A.V.: 1989, *Radioastronomicheskaya apparatura. Thes. of the XXI All Union Conference.* Erevan. 109.

Golubchina O.A., Golubchin G.S.: 1981, *Astrofiz. issled. (Izv. SAO),* **14**, 125.

Golubchina O.A., Golubchin G.S.: 1983, *Radiofizika*, **26**, 1472.

Gregory P.C., Condon J.J.: 1990, *Prepr. NRAO* 90/91, 1.

Hewitt A., Burbidge G.: 1987, *Astrophys.J. Suppl.Ser.*, **63**, 1.

Hewitt A., Burbidge G.: 1989, *Astrophys.J. Suppl.Ser.*, **69**, 1.

Hjellming R.M.: 1989, in: *Synthesis Imaging in Radio Astronomy. A Collection of Lectures from the Third NRAO Synthesis Imaging Summer School.* Eds.: R.A.Perley, F.R. Schwab, A.H. Bridle. Astron. Soc. of Pacific. 477.

Hogbom J.A.: 1974, *Astron. Astrophys. Suppl. Ser.*, **15**, 417.

Ivanov L.N.: 1979, *Astrofiz. issled. (Izv. SAO)*, **11**, 213.

Kaidanovskij N.L.: 1982, *Astrofiz. issled. (Izv SAO)*, **16**, 100.

Khaikin S.E., Kaidanovskij N.L.: 1959, *Pribory i tekhnika eksperimenta*, **2**, 19.

Khaikin S.E., Kaidanovskij N.L., Esepkina N.A., Korolkov D.V., Parijskij Yu.N., Stotskij A.A., Shakhbazyan Yu.L., Shivris O.N.: 1967, *Izvestiya GAO USSR AS*, L.

182, 235.

Korolkov D.V., Fridman P.A.: 1970, *Astrofiz. issled. (Izv. SAO)*, **2**, 148.

Korolkov D.V., Majorova E.K., Stotskij A.A.: 1978, *Astrofiz. issled. (Izv. SAO)*, **10**, 85.

Kuznetsova G.V., Soboleva N.S.: 1964, *Izvestiay GAO USSR AS*, L., **172**, 122.

Kuznetsova G.V.: 1973, *Astrofiz. issled. (Izv. SAO)*, **5**, 150.

Lebed V.I., Yaryomenko A.V.: 1985, *Radioastronomicheskaya apparatura. Thes. of the XVII All Union Conference.* Erevan. 264.

Majorova E.K., Stotskij A.A.: 1986, *Astrofiz. issled. (Izv. SAO)*, **22**, 119.

Majorova E.K., Nizhelskij N.A., Trushkin S.A., Tsybulev P.G.: 1993, *Bull.Spec. Astrophys.Obs.*, **35**, 148..

Minchenko B.S.: 1977, *Astrofiz.issled. (Izv. SAO)*, **9**, 29.

Minchenko B.S.: 1978, *Astrofiz.issled. (Izv. SAO)*, **10**, 99.

Minchenko B.S.: 1979, *Ph.D. Thesis, GAO USSR AS,* Leningrad.

Minchenko B.S.: 1986, *Astrofiz.issled. (Izv. SAO)*, **21**, 91.

Mingaliev M.G., Petrov Z.E., Filipenko V.I., Cherkov L.N.: 1985, *Astrofiz. issled. (Izv. SAO)*, 1985, **19**, 76.

Mingaliev M.G.: 1985, *Ph.D. Thesis,* SAO USSR AS, Nizhnij Arkhys.

Mingaliev M.G., Verkhodanov O.V., Khabrakhmanov A.R., Golnev B.Ya., Temirova A.V.: 1991, *Soobshch. Spets. Astrofiz. Obs.*, **68**, 47.

Parijskij Yu.N.: 1961. *Ph.D. Thesis,*GAO USSR AS, Leningrad.

Parijskij Yu.N.: 1969. *Doctor of Science Thesis,* GAO USSR AS, Leningrad.

Parijskij Yu.N., Shivris O.N.: 1972, *Izvestiya GAO USSR AS*, L., **188**, 13.

Parijskij Yu.N., Korol'kov D.V.: 1986, *Itogi nauki i tekhniki. Seriya Astronomiya.* Moscow: VINITI. **31**, 73.

Parijskij Yu.N.: 1986, *Prepr.* No.33L. SAO USSR AS. Leningr. branch.

Parijskij Yu.N., Verkhodanov O.V.: 1993, *Prepr.* No. 90 SPb., SAO RAS, St.Petersburg branch.

Perley R.A., Dreher J.W., Cowan J.T.: 1984, *Astrophys.J.*, **285**, L35.

Pinchuk G.A., Stotskij A.A.: 1982, *Astrofiz. issled. (Izv. SAO)*, **16**, 135.

Pinchuk G.A., Parijskij Yu.N., Shannikov D.V., Majorova E.K.: 1989, *Prepr.* No. 39. SAO RAS, Nizhnij Arkhyz.

Shennon K.: 1963. *Raboty po teorii informatsii i kibernetike.* USSR. IL.

Shivris O.N., Postoenko Yu.K., Trunov V.V.: 1983, *Astrofiz. issled. (Izv. SAO)*, **17**, 84.

Soboleva N.S., Temirova A.B., Pyatunina T.B., Shivris O.N., Vitkovskij V.V., Plyaskina T.A., Shergin V.S.: 1986, *Prepr.* No. 32L, SAO USSR AS, Leningr. branch.

Stotskij A.A.: 1972, *Izvestiya GAO USSR AS*, L., **188**, 63.

Stotskij A.A., Kalikhevich G.N., Osina T.N., Pinchuk G.A.: 1987, *Astrofiz. issled. (Izv. SAO)*, **25**, 143.

Terebizh V.Yu.: 1990, *Astrofizika*, **32**, 327.

Thompson A.R., Clark B.G., Wade C.M., Napier P.J.: 1980, *Astrophys.J. Suppl.Ser.* 151.

Verkhodanov O.V., Erukhimov B.L., Monosov M.L., Chernenkov V.N., Shergin V.S.: *Prepr.* No. 89, SAO RAS, Niznij Arkhys.

Verkhodanov O.V., Vitkovskij V.V., Erukhimov B.L., Zhelenkova O.P., Likhvan O.P. nosov M.L., Chernenkov V.N., Shergin V.S.: 1993, *Prepr.* No. 89 SPb, SAO St.Petersburg branch.

Verkhodanov O.V.: 1993. *Ph.D. Thesis,* SAO RAS, Nizhnij Arkhys.

Verkhodanov O.V.: 1993a. *Prepr.* No. 91 SPb, SAO RAS, St. Petersburg.

Wells D.C, Greisen E.W., Harten R.H.: 1981, *Astron. Astrophys. Suppl.Ser.*, **44**,

Wild: 1969, *Proc. IRE.* Austr., **28**, 9.

Received 1993 August 10